NASA CR - 135319

ADVANCED CERAMIC MATERIAL FOR HIGH TEMPERATURE TURBINE TIP SEALS

(NASA-CR-135319) ADVANCED CERAMIC MATERIAL FOR HIGH TEMPERATURE TURBINE TIP SEALS Interim Technical Progress Report, Feb. 1976 - Nov. 1977 (International Harvester Co.) 60 p HC A04/MF A01 CSCL 11B G3/27

N78-31238

Unclas 31686

INTERIM TECHNICAL PROGRESS REPORT NO. 1

by

N.G. Solomon, J.W. Vogan and A.R. Stetson

Solar Division of International Harvester Company
San Diego, California

Period: February 9, 1976 to October 31, 1977

Contract NAS3-20081

Prepared For

National Aeronautics and Space Administration
Lewis Research Center
21000 Brookpark Road
Cleveland, Ohio 44135

FOREWORD

This Interim Technical Report covers the work performed under Contract NAS3-20081 from February 9, 1976 to October 31, 1977. It is published for technical information only and does not necessarily represent recommendations, conclusions, or approval of NASA-Lewis Research Center.

Contract NAS3-20081, with Solar Turbines International, an Operating Group of International Harvester Company, San Diego, California, is sponsored by the NASA-Lewis Research Center with Mr. Stanley Young as the Program Manager.

The program is being conducted at Solar Turbines International with Mr. J. W. Vogan as the Principal Investigator. Mr. A. R. Stetson is the Solar Program Technical Director.

Solar's internal report number is RDR 1831-23.

A. R. Stetson, Chief
Materials Engineering
12/19/77
Date

N. G. Solomon
Research Engineer
12/19/77
Date

W. A. Compton
Director-Research
12-20-77
Date

J. W. Vogan
Senior Research Engineer
12/19/77
Date

PRECEDING PAGE BLANK NOT FILMED

SYNOPSIS

- This effort was initiated by NASA as an exploratory test program to evaluate ceramic materials for use as abradable gas path seals in turbine engines at temperatures up to 1370°C.
- Silicon nitride and silicon carbide compositions of varying densities and structures were evaluated using Bradelloy 500 as a baseline material.
- Honeycomb type silicon nitride and low density silicon carbide have been recommended to NASA for further study.
- Tests with silicon nitride blade tips demonstrated that they had desirable rub characteristics.
- The initial contract was revised to broaden its scope and exploit results of the initial test program.

Key Words: Ceramics, Seals, Abradables, High Temperature Seals, Ceramic Bonding, Blade Tip Inserts, Turbine Tip Seals, Silicon Carbide, Silicon Nitride, Turbine Blade Tip Sealing.

SUMMARY

Forty-four ceramic material systems were considered for potential use as turbine blade tip gas path seals at temperatures up to 1370°C. The selected systems were limited to silicon carbide and silicon nitride structures since an initial analysis of the problem gave these materials the greatest potential for development into a successful materials system. Not all of the desired structures were available for testing.

Silicon nitride and silicon carbide materials over a range of densities (processed by various methods) and a honeycomb structure of silicon nitride were obtained as were ceramic blade tip inserts fabricated from both materials by hot pressing. These were tested singly and in combination. The evaluations included wear under simulated engine blade tip rub conditions, thermal stability, impact resistance, machinability, hot gas erosion and feasibility of fabrication into engine components.

The silicon nitride honeycomb and low-density silicon carbide using a selected grain size distribution gave the most promising results as rub-tolerant shroud liners and will be subject to further development. Reaction-bonded silicon nitride materials (20-60 percent dense) failed in test, as did similar components made from fine grained silicon carbide. Ceramic blade tip inserts made from hot-pressed silicon nitride gave excellent test results. Their behavior closely simulated metal tips. They did not severely fracture during rub. Wear was similar to that of metals but reduced by a factor of six. Analytical studies of the feasibility of incorporating ceramic tips into metal blades are now in progress.

The results to date have demonstrated that honeycomb type silicon nitride structures and low density silicon carbide structures should undergo further testing and evaluation. At the same time, problem areas were identified that needed additional study. These problem areas were: attachment to the substructure, material optimization, the effect of variations in rub parameters and the feasibility of using ceramic tips on turbine blades. Therefore, the original program plan was revised to broaden its scope and submitted to the NASA Program Manager.

TABLE OF CONTENTS

Section			Page
1	INTRODUCTION		1
2	TEST PROGRAM		3
	2.1	Test Procedures	3
		2.1.1 Oxidation Resistance	7
		2.1.2 Ballistic Impact	7
		2.1.3 Abradability	7
		2.1.4 Hot Gas Erosion and Hot Abradability	8
	2.2	Experimental Results	9
		2.2.1 Characterization of Materials	9
		2.2.2 Oxidation Testing	10
		2.2.3 Abradability Testing	
		2.2.4 Ballistic Impact Test	27
		2.2.5 Hot Gas Erosion Testing	27
	2.3	Conclusions and Recommendations	34
APPENDICES			
A	BALLISTIC IMPACT TESTING EQUIPMENT		37
B	ABRADABILITY TESTING RIG		41
C	OXIDATION/EROSION RIG		49

LIST OF ILLUSTRATIONS

Figure		Page
1	Flow Chart of the Revised Testing Program	5
2	Flow Chart of the Original Task I - Screening Tests	6
3	Effect of Elevated-Temperature Testing on Low Density Silicon Carbide Abradables	12
4	Effect of Elevated-Temperature Oxidation Testing on Low Density Silicon Nitride Abradables	13
5	2 mm Cell Unfilled Honeycomb Silicon Nitride Before Oxidation Test	15
6	2 mm Cell Unfilled Honeycomb Silicon Nitride After 500 Hours Oxidation Test at 1370°C	15
7	2 mm Cell Filled Honeycomb Silicon Nitride Before Oxidation Test	15
8	2 mm Cell Filled Honeycomb Silicon Nitride After 500 Hours Oxidation at 1370°C	16
9	Nodal Joints of 2 mm Cell Filled Honeycomb Silicon Nitride After 500 Hours Oxidation at 1370°C	16
10	Oxide Layer Formed on 2 mm Cell Filled Honeycomb Silicon Nitride After 500 Hours Oxidation at 1370°C	16
11	Bradelloy 500 Specimen After Oxidation Test at 1370°C for 2 Hours	17
12	Silicon Carbide, 60 Percent Dense, 100/60 Mesh, After Rub Testing	19
13	Silicon Carbide, 50 Percent Dense, 320 Mesh, After Rub Test	19
14	Reaction Bonded, 60 Percent Dense, Silicon Nitride After Rub Test	20
15	Sintered, 60 Percent Dense, Silicon Nitride After Rub Test	20
16	2 mm Honeycomb Silicon Nitride After Rub Test	21
17	MAR-M421 Blade Tip After Test Rub on Silicon Nitride Honeycomb	21
18	End View of MAR-M421 Blade After Rub Test	22
19	Silicon Nitride Blade Tip Profile After Rub Test	22

LIST OF ILLUSTRATIONS (CONT)

Figure		Page
20	Silicon Nitride Blade Tip After Rub Test	22
21	Silicon Carbide Blade Tip After Rub Test	24
22	Silicon Carbide Blade Tip After Rub Test	24
23	Typical Section of a Silicon Carbide Blade Tip After Test	24
24	Silicon Carbide Tip Profile After Rub on 60/100 Mesh Silicon Carbide, 60 Percent Dense	25
25	Silicon Carbide Tip After Rub on 60/100 Mesh Silicon Carbide, 60 Percent Dense	25
26	Bradelloy, Penetration Rate, 0.050 mm/sec	26
27	Bradelloy, Penetration Rate, 0.025 mm/sec	26
28	Bradelloy, Penetration Rate, 0.012 mm/sec	26
29	Silicon Nitride 40 Percent Dense After Impact Test	29
30	Silicon Carbide 40 Percent Dense After Impact Test	29
31	Silicon Nitride 60 Percent Dense After Impact Test	30
32	Silicon Carbide 60 Percent Dense After Impact Test	30
33	Filled 1 mm Cell Silicon Nitride After Impact	31
34	Unfilled 2 mm Honeycomb Silicon Nitride After Impact Test	31
35	Unfilled 1 mm Honeycomb Silicon Nitride After Impact Test	31
36	1 mm Cell Unfilled Honeycomb Silicon Nitride Before Erosion Test	32
37	1 mm Cell Filled Honeycomb Silicon Nitride After 100 Hours Hot Gas Erosion	32
38	1 mm Cell Unfilled Honeycomb Silicon Nitride After 100 Hours Hot Gas Erosion	32
39	Reaction Bonded Silicon Nitride After Hot Gas Erosion Test Showing Cracking Due to Particle Impact	33
40	Reaction Bonded Silicon Nitride After Hot Gas Erosion Test Showing Crack Propagation From Impact Crater	33
41	Reaction Bonded Silicon Nitride After Hot Gas Erosion Showing Glassy Phase on Surface	33
42	Typical Laboratory Setup for Impacting Ceramic Specimens	39

LIST OF ILLUSTRATIONS (CONT)

Figure		Page
43	Schematic of Seal Test Rig	44
44	Seal Test Rig Wheel Showing MAR-M421 Alloy Stub Blades	45
45	Seal Test Rig Showing Location of Test Seal Material	46
46	Seal Test Rig Showing Setup for Testing Honeycomb Blade Tip Seals at Elevated Temperature	47
47	Typical Abradable Seal Sample	48
48	Oxidation/Erosion Rig	51

LIST OF TABLES

Table		Page
1	Material Systems Variation - Level Sets	4
2	Average Bulk Density of Ceramic Abradables	11
3	Room Temperature Abradable Rub Tests	18
4	Ballistic Impact Test Results at Ambient Temperature (Velocity 127 mps, Impingement Angle 30 Degrees, 4.78 mm Steel Spheres)	28
5	Test Parameters for Abradability Tests	36

UNIT CONVERSION

Modern Metric (SI)	English
356.0 mm	14.0 inch
216.0 mm	8.5 inch
50.0 mm	2.0 inch
25.0 mm	1.0 inch
6.4 mm	0.25 inch
5.0 mm	0.2 inch
4.78 mm	0.188 inch
3.0 mm	0.12 inch
2.0 mm	0.08 inch
1.3 mm	0.05 inch
1.0 mm	0.04 inch
0.91 mm	0.036 inch
0.76 mm	0.03 inch
0.025 mm	0.001 inch
550.0 m/sec	1804 ft/sec
427.0 m/sec	1400 ft/sec
305.0 m/sec	1000 ft/sec
127.0 m/sec	416 ft/sec
0.012 mm/sec	0.0005 in./sec
0.05 mm/sec	0.002 in./sec
1370°C	2500°F
1200°C	2192°F
426 °C	799°F
0.440 gms	0.016 oz
1.4 Kg/sec	0.02 lb/sec
0.07 Kg/mm^2	100 $lb/in.^2$

1

INTRODUCTION

The problem generated by high speed turbine blade tips moving in close proximity to the outer case has been resolved in numerous ways by designers. The earliest approach was to provide sufficient clearance between the tip of the turbine blade and the outer shroud so that rubs did not occur during any phase of the turbine operation. The clearance required is large since provision must be made for transient temperature differentials during startup, acceleration, shut down, hot restart and violent maneuvers. Tolerance stackup and other factors also contribute to the problem. To reduce tip clearance requirements and prevent blade tip wear during rub, a stable high temperature abradable tip shoe is needed. Because of the high temperatures involved, and the need for high rub tolerance, low apparent density ceramic materials are logical candidates as are open structures similar to metal honeycomb.

This program was established by NASA to select and develop ceramic material systems for use as turbine tip seals operating at temperatures up to 1370°C. Silicon carbide and silicon nitride were selected as the two most logical starting materials for this application. A total of 44 material systems were selected during the program. To aid in evaluation, a currently used shroud material, Bradelloy 500, was proposed as a baseline material throughout the initial program. It was to be subjected to the same tests as the candidate materials. Quantitative test results were to be related to the baseline material.

The program was divided into three tasks. Task I consisted of a material screening test program. This screening program included thermal stability tests, hot gas erosion tests, ambient temperature abradability testing, abradability testing at 1370°C and ballistic impact tests. The results of these tests were to be used to recommend a material system for advanced laboratory evaluation in Task II. Thermal and physical properties of the selected material were to be determined at this time as a basis for engineering design. Progress to date is described in this interim report.

2

TEST PROGRAM

The test program is designed to isolate a material system satisfying the operating requirements for a ceramic seal system as listed below.

1. Thermal and chemical stability in an oxidizing atmosphere at temperatures up to 1370°C.
2. Resistance to thermal shock without cracking or loss of material.
3. Rub tolerance with minimal blade wear.
4. Impact resistance to prevent gross failure from foreign objects in the gas stream at temperatures up to 1370°C.
5. Dimensional stability to retain attachment integrity and, to a lesser extent, to maintain seal clearances.

The materials systems selected for this requirement are presented in Table 1. The system numbers are used to identify the materials used in the test program.

A second requirement is to establish design criteria for incorporating the selected seal system into an existing engine. A flow chart combining initial efforts and a revised program to meet these objectives is given in Figure 1. Testing is designed to produce both quantitative data and a comparison with materials currently in use.

2.1 TEST PROCEDURES

Two applications of materials, wear resistant blade tips and abradable shroud structures, were screened prior to selecting a material system for advanced evaluation. Oxidation resistance, ballistic impact resistance, and abradability at room temperature were used for initial screening tests. Selected materials were then subjected to hot gas oxidation/erosion testing and hot abradability tests.

Figure 2 shows a flow chart of the Task I testing program, and specific test procedures are described in the following paragraphs.

Table 1

Material Systems Variation -Level Sets

Material System Number	Seal Description			Blade Tip
1*	Corrugated from plasticized Si_3N_4	3 mm cell height		MAR-M421
2		2 mm cell height		
3		1 mm cell height		
4*	Corrugated from plasticized Si_3N_4	3 mm cell height	Silicon powder fill and nitride	MAR-M421
5		2 mm cell height		
6		1 mm cell height		
7*	Corrugated from plasticized Si_3N_4	Select best three from material systems No. 1	1 mm Si_3N_4	Ceramic tip
8			2 mm Si_3N_4	
9			Filled Si_3N_4	
10	Reaction bonded Si_3N_4	60 percent dense		MAR-M421
11		50 percent dense		
12		40 percent dense		
13	Reaction bonded Si_3N_4	60 percent dense		Ceramic tip
14		50 percent dense		
15		40 percent dense		
16	Silicon Carbide 320 Mesh	60 percent dense		Ceramic tip
17		50 percent dense		
18		40 percent dense		
19*	Hollow SiC spheres spheres in chemical vapor deposited silicon carbide matrix.	50 percent dense		MAR-M421
20*		40 percent dense		
21*		30 percent dense		
22	Silicon carbide 100/60 Mesh	60 percent dense		Ceramic tip
23		50 percent dense		
24		40 percent dense		
25	Silicon carbide 100/60 Mesh	60 percent dense		Ceramic tip
26		50 percent dense		
27		40 percent dense		
28	Silicon carbide 100/60 Mesh	60 percent dense		MAR-M421
29		50 percent dense		
30		40 percent dense		
31	Silicon carbide 100/60 Mesh	60 percent dense		MAR-M421
32		50 percent dense		
33		40 percent dense		
34	Si_3N_4 100-150 Mesh			MAR-M421
35	Reaction bonded	60 percent dense		Ceramic tip
36	Si_3N_4 Sintered	60 percent dense		MAR-M421
37				Ceramic tip
38*	SiC graded structure abradable to solid bonding			MAR-M421
39*				Ceramic tip
40	Corrugated Si_3N_4	(2mm cell size)	Open	Thin M421 tip
41			Filled	Ceramic tip
42	Corrugated Si_3N_4	(1mm cell size)	Filled	Ceramic tip
43	Bradelloy 500		Baseline	MAR-M421
44				Ceramic

* Proposed vendor unable to supply and alternate source could not be located.

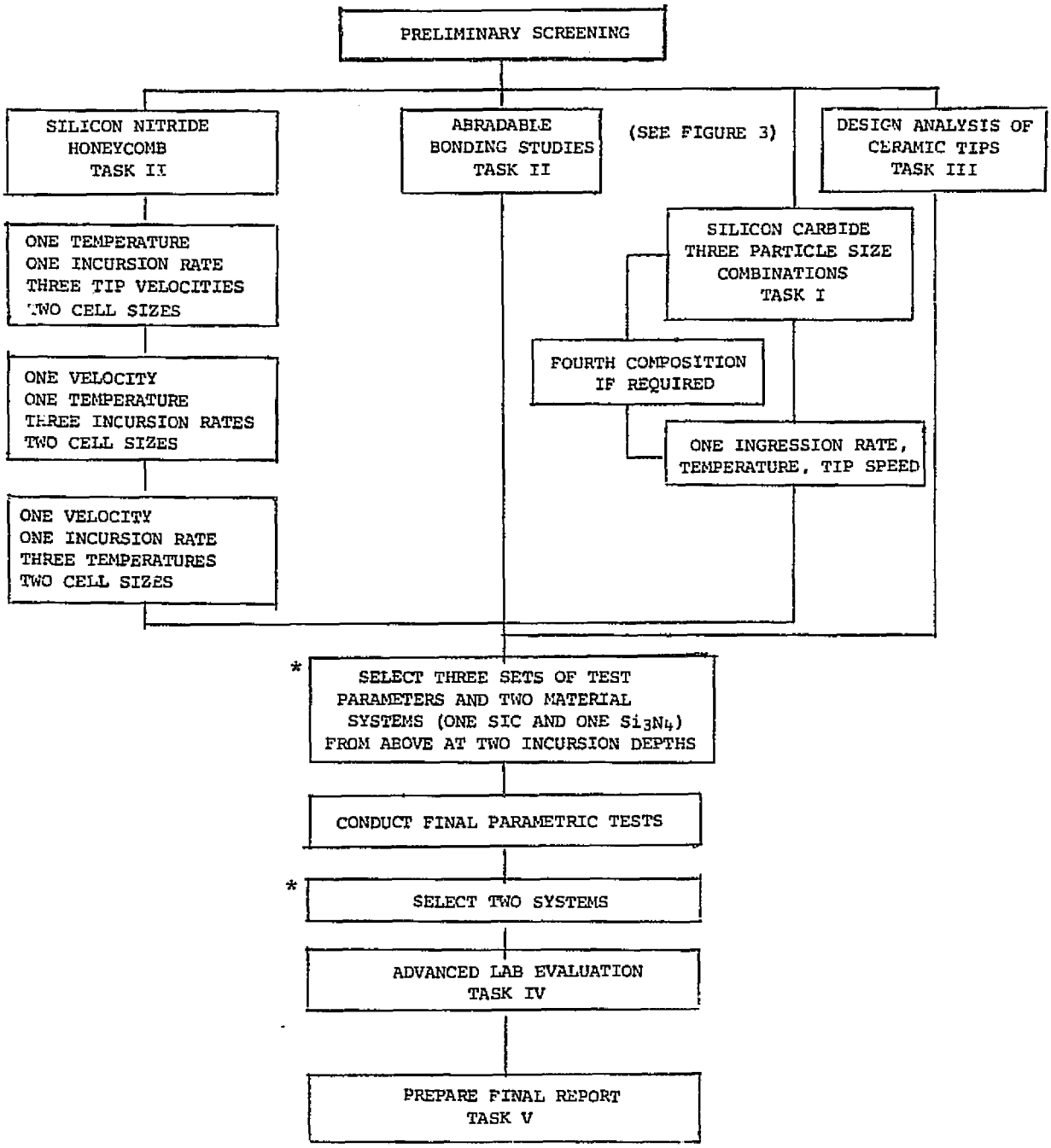

* NASA CONCURRENCE REQUIRED AT THESE POINTS

Figure 1. Flow Chart of the Revised Testing Program

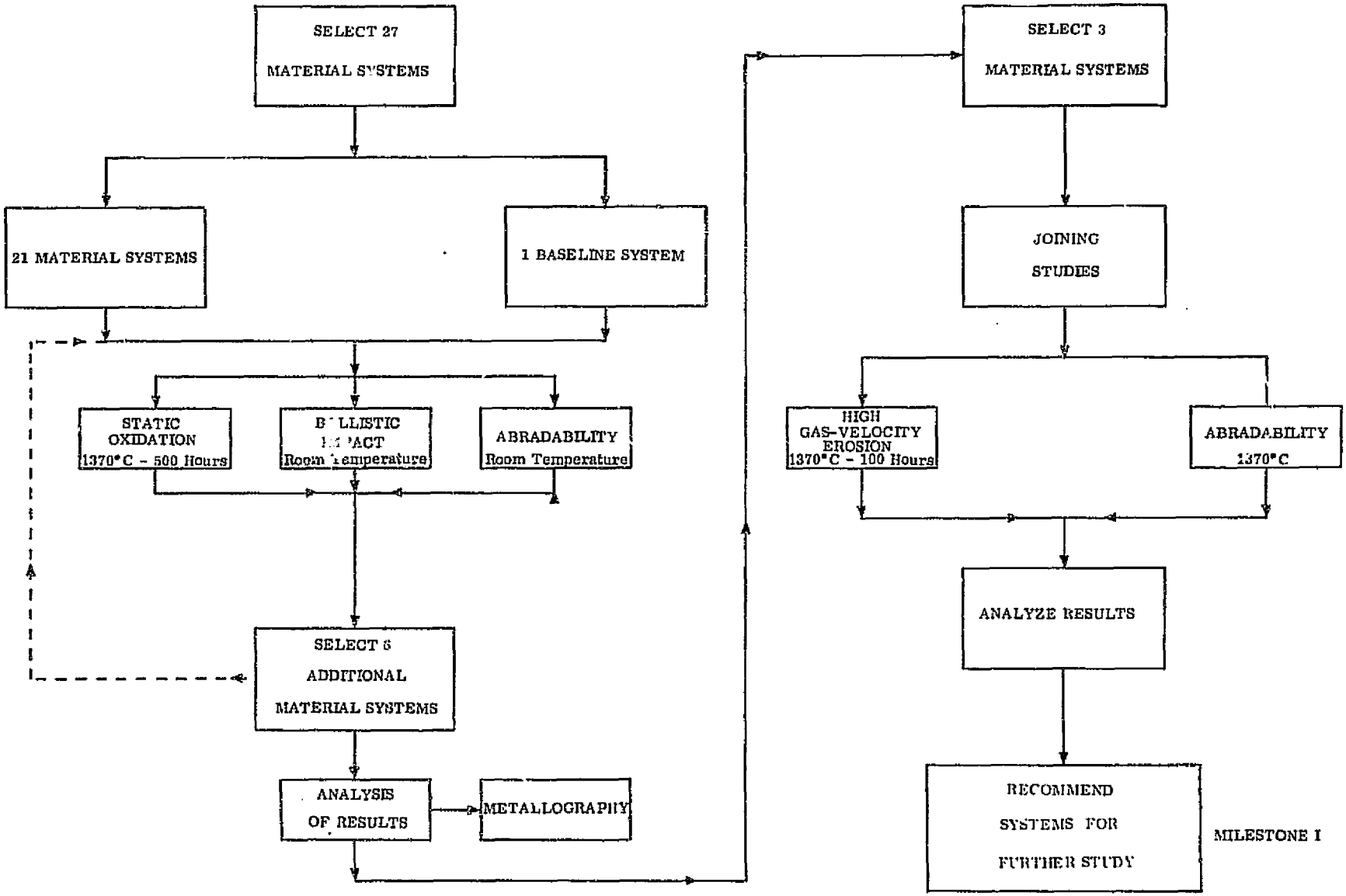

Figure 2. Flow Chart of the Original Task I - Screening Tests

2.1.1 Oxidation Resistance

Samples, 25 mm by 25 mm by 5 mm, were weighed, measured and placed in an electric furnace preheated to 1370°C with static air as the atmospheric environment. After 50 hours exposure the samples were removed from the furnace, cooled to room temperature and weighed. They were then returned to the furnace for an additional 50 hours exposure and the measurements duplicated. The cycle was then repeated every 100 hours until a total of 500 hours exposure was reached. At completion of the test, weight change data was evaluated and extrapolated to indicate the probable results of a 10,000-hour exposure.

In addition, the samples were examined visually for cracking, warping or other evidence of failure each time they were removed from the furnace. Sections were prepared of each material for metallographic examination after 500 hours exposure and compared with samples taken from each material prior to test.

2.1.2 Ballistic Impact

The test materials were evaluated for ballistic impact resistance as follows. Each specimen was adhesively bonded to a steel backing and then placed in the ballistic impact test facility (Appendix A) to give an impact angle of 30 degrees. The equipment was standardized at an impact velocity of 127 mps using a steel ball 4.78 mm in diameter with a mass of 0.440 gms. After test the specimens were examined for impact damage (typically cracking, material loss) and the systems ability to withstand foreign object impact during engine operation.

2.1.3 Abradability

Abradability of the materials was initially performed at room temperature. Samples of each composition (50mm x 50mm x 5mm) were adhesively bonded to a steel support fixture and machined to a 21.6 cm radius. Both grinding and single point machining were used. The single point machining proved to be the most effective with these materials. Solar turbine blades fabricated from MAR-M421 alloy were used in the turbine disc for these abradability tests. These blades were mounted in the disc and ground to a length of 6.4 mm for windage control.

During test, shear forces acting on the test sample (as characterized by the stress on the instrumented sample support and measured with strain gages) and the sample temperature rise (monitored by a thermocouple located 1.3 mm beneath the initial center of rub) were automatically recorded. After testing, blade wear was measured and the appearance of the tip observed. Wear and relevant changes in the abradable materials were also determined.

Representative metallurgical specimens were prepared from both the blades and test specimens for metallurgical examination. From these data overall performance was evaluated for the material under test.

The abradability test parameters were as follows:

- Temperature: ambient (≈82°C due to air friction)
- Blade velocity: 427 mps
- Incursion rate: 0.025 mm per second
- Depth of rub: 0.76 mm

A detailed description of this test facility can be found in Appendix B together with a sketch depicting a typical test specimen.

2.1.4 Hot Gas/Erosion and Hot Abradability

When oxidation, abradability, and ballistic impact tests were completed, the most promising systems were then tested at elevated (1370°C) temperatures for gas erosion and abradability.

Hot Gas Erosion Tests

The test facility was operated with kerosene fuel and preheated air. Combustion products at a velocity of 550 mps was directed onto the sample at an impingement angle of 30 degrees to the sample surface. During test the sample surface temperature was monitored optically and the burner adjusted to maintain it at 1370°C. Additional data was obtained by thermocouples located 6.4 mm beneath the initial sample surface. This temperature data was used to maintain reproducible test conditions.

After testing for 100 hours, sample weight change, the depth of the erosion and the area over which the sample was eroded was measured. The relative erosion characteristics were recorded for each material and compared with the results obtained when the baseline material was tested in the same manner.

Appendix C provides a description of the hot gas erosion test facility.

High Temperature Abradability

Further evaluation of abradable seal material systems was performed on the rub test rig. These tests were similar to those conducted at room temperature except that the sample temperature was stabilized at 1370°C prior to test.

As in the previous testing, temperature rise due to rub in the sample was recorded throughout the test, as was the stress on the abradable sample. Temperature monitoring of the sample was accomplished by a thermocouple located 1.3 mm beneath the initial rub surface. The baseline material was not tested at 1200°C as originally planned since data from other tests indicated that the material was not stable in this environment and severe equipment damage might occur. Metallurgical sections were prepared after test to detect any changes in the material resulting from the test.

2.2 EXPERIMENTAL RESULTS

All of the material systems (see Table 1 for system identification) were evaluated except for the 3 mm cell silicon nitride honeycomb (systems 1 and 4), the chemical vapor deposited hollow silicon carbide spheres (systems 19 thru 21), and the graded silicon carbide structures (systems 38 and 39).

The following sections detail results of Phase I screening tests.

2.2.1 Characterization of Materials

Upon receipt, each test material was weighed and measured. This data was used to calculate its apparent density. Metallurgical sections were also prepared to establish its initial structure for evaluation at this time and determination of changes occurring during test. Results of the density calculations are reported in Table 2. The systems with which each material was evaluated can be identified by reference to Table 1. The value of 3.44 gm/cc (Handbook of Chemistry and Physics, 49th edition) is used as the basis for calculating relative densities. For comparison purposes only, the honeycomb structures were treated as a homogeneous structure. Subsequent measurements showed the reaction bonded ribbon used in their manufacture had a density of 80 percent (2.8 gm/cc) of the literature value. Filling the openings increased its bulk density by 33 percent (1.14 gm/cc) of theoretical density. Silicon carbide materials very closely approached specified values. These were based on a theoretical density of 3.217 gms/cc (ibid). Two types were received as indicated in Table 2. The first was manufactured from a -325 mesh powder and the second from a combination of -100 and -60 mesh material. The -325 materials were less uniform in structure than their coarse grained counterparts. Evidence of high and low density areas were observed as striations in the material. The coarser grained structure was uniform in appearance.

Obtaining silicon nitride materials in a range of densities was less successful. Materials approaching the value 60 percent dense requirement were readily obtained. These had a uniform fine grained structure. Materials specified to a lower bulk value were not obtainable in a constant quality and most vendors were unwilling to quote on supplying them. Those that were obtained were far below the desired density. Typical values for the received material lay in the neighborhood of 20 percent of theoretical density, about half of the specified minimum value.

In addition to the low density silicon nitride materials, three other ceramic abradables could not be obtained as noted at the beginning of this section. These were:

1. Silicon nitride honeycomb (3 mm cell)
2. Graded silicon carbide structures
3. Hollow silicon carbide spheres

These were deleted from the program after contacting several vendors and establishing that the development effort required for their production was beyond the scope of the current program.

Bradelloy 500 was obtained in the form of brazed structures attached to a Hastelloy X backing. Because of this structure, useful density data was not attempted. Metallurgical specimens were prepared and are included in the relevant sections of this report where they are used as the basis for detecting material changes resulting from testing under various conditions.

2.2.2 Oxidation Testing

All of the materials listed in Table 2 were tested for 500 hours in static oxidation at 1370°C.

The results of these tests are shown graphically in Figures 3 and 4. The data is plotted on the basis:

$$x = k\ (\log[t])$$

where:

x = percent weight increase
t = exposure time (hours)
k = rate constant

A significant difference was observed in the response of silicon nitride and silicon carbide that related to basic composition rather than to the structure under test. The structures based on silicon nitride showed a rapid rate of oxidation during the first 50 hours of test. This rate dropped to a low constant value for the remainder of the test.

It was also observed that as density decreased the rate of oxidation increased with a very rapid rate of oxidation occurring in the 20 percent dense material. In evaluating these tests results, a value of 80 percent (the ribbon density) should be used for the honeycomb silicon nitride structures. Hot-pressed silicon nitride samples showed very low weight gain when tested in this manner.

Table 2

Average Bulk Density of Ceramic Abradables

Material System(s)*	Material	Density (gms/cc)	Percent Theoretical Density	
			Specified	Actual
3 and 6	Corrugated Silicon Nitride 1 mm Cell Size	0.823	None	23.9
2 and 5	Corrugated Silicon Nitride 2 mm Cell Size	0.697	None	20.3
25, 26 & 27	Hot Pressed Silicon Carbide	3.22	100	100
22 and 25	Silicon Carbide 100/60 Grit	2.00	60	62.2
23 and 26	Silicon Carbide 100/60 Grit	1.60	50	49.7
24 and 27	Silicon Carbide 100/60 Grit	1.28	40	39.8
16	Silicon Carbide 320 Grit	1.99	60	61.8
17	Silicon Carbide 320 Grit	1.64	50	51.0
18	Silicon Carbide 320 Grit	1.32	40	41.0
10 and 13	Silicon Nitride	2.18	60	63.4
12 and 15	Silicon Nitride	0.727	40	21.1
5	Filled Silicon Nitride (0.08) cell size)	1.11	None	32.3
6	Filled Silicon Nitride (0.04 cell size)	1.09	None	31.7
34	Silicon Nitride 100-150 grit (reaction bonded)	1.95	60	57.3
36	Sintered Silicon Nitride	2.25	60	66.6

*See Table 1

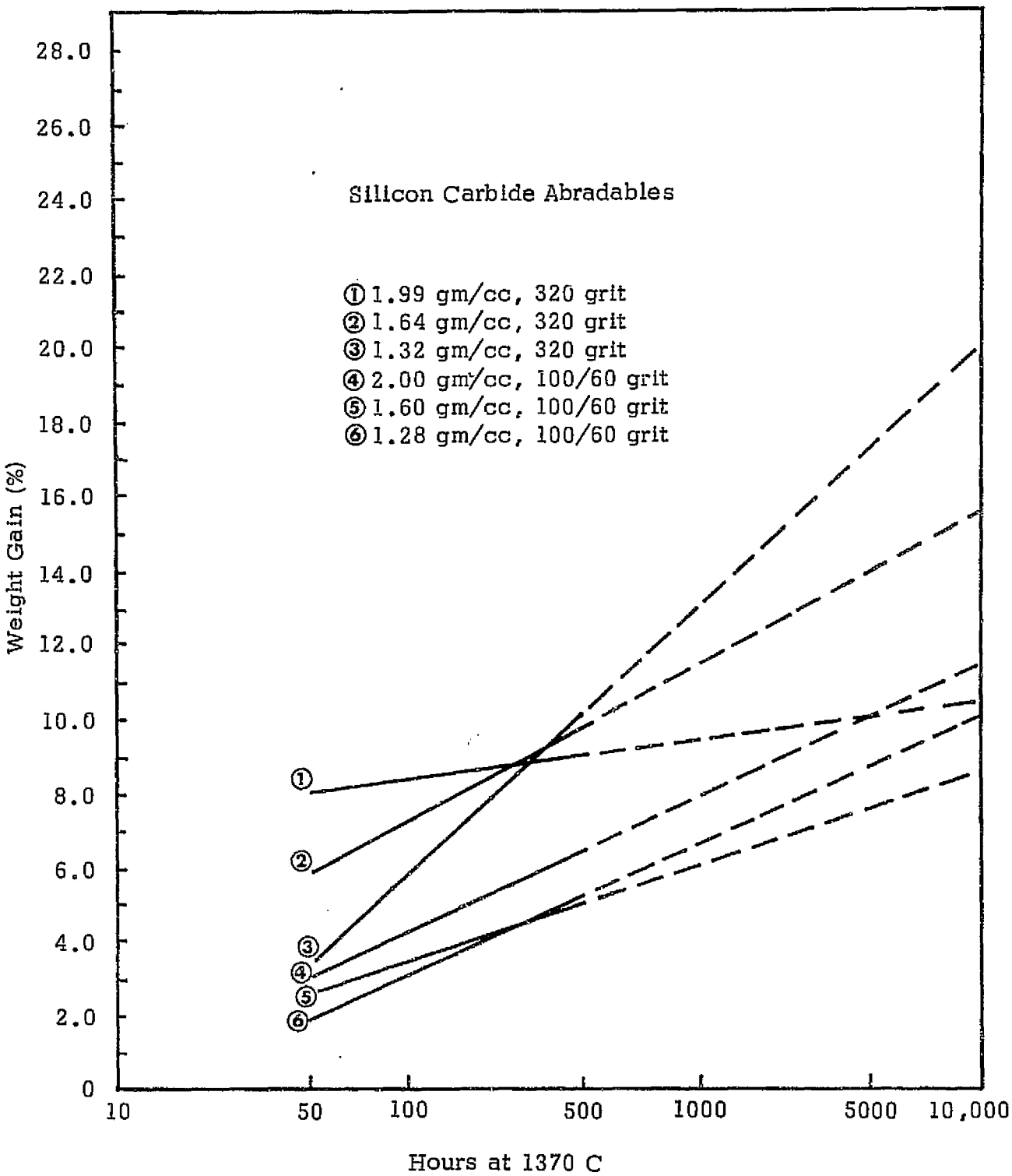

Figure 3. Effect of Elevated-Temperature Testing on Low Density Silicon Carbide Abradables

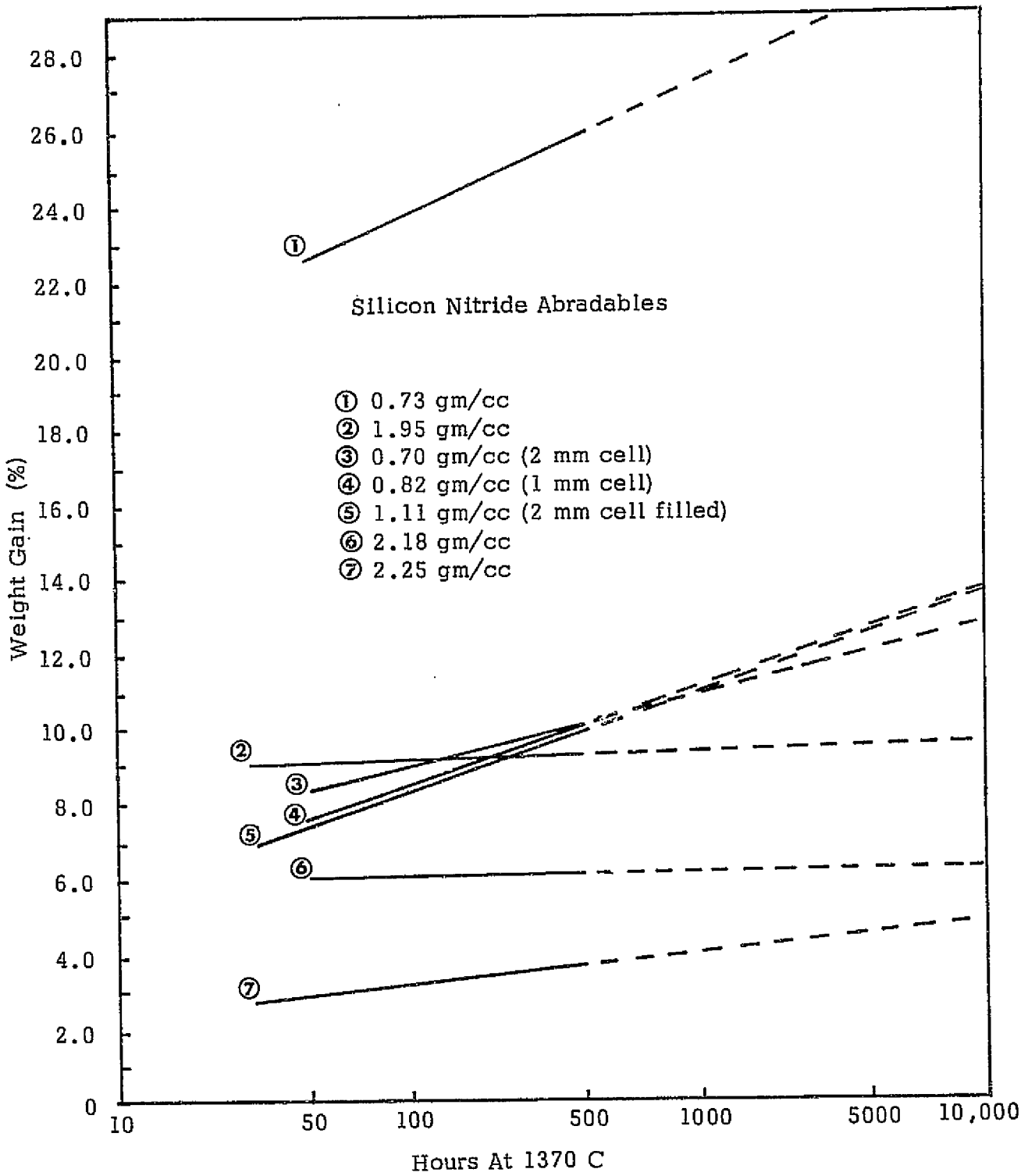

Figure 4. Effect of Elevated-Temperature Oxidation Testing on Low Density Silicon Nitride Abradables

Photographs of filled and unfilled silicon nitride honeycomb samples before and after oxidation are shown in Figures 5 through 10. There was little visual difference between filled and unfilled samples after oxidation. Both samples showed a glassy silica phase on exposed surfaces as well as penetration of the oxide layer into the nodal joints of the corrugated layers. Oxide penetration into the nodal joints was reduced in the filled samples. Migration to the surface by the silicon nitride-glass filler material to form a protective layer for the honeycomb was observed. However, in many cases, the migration of material also resulted in a mechanical breakdown of the nodal joint.

In contrast to the silicon nitride materials, structures based on silicon carbide had a nearly constant rate of oxidation during the test. The fine grained, low density samples showed the least stability during test. Coarse grained samples were less affected (100/60 mesh) particularly in the 60 percent dense material. The fully dense blade tips were little affected by exposure in air at 1370°C and no significant changes were detected as a result of the test.

Bradelloy 500 was also subjected to a 1370°C oxidation test. After two hours, the Hastelloy X honeycomb had deteriorated to the point where the physical integrity of the sample was lost (Fig. 11).

2.2.3 Abradability Testing

Nineteen material systems have been tested for ambient temperature abradability. Sixteen of these tests used MAR-M421 blades. Three were conducted using ceramic tipped blades (hot pressed silicon nitride and silicon carbide). The room temperature test results are summarized in Table 3.

The rub tolerance of silicon carbide abradables was highly dependent upon grain size and density. Fine grained (-325 mesh) materials tended to wear blade tips and were susceptible to thermal shock. Large grained materials (60/100 mesh) formed structures with easily dislodged grains which eroded adjacent areas by high velocity particle impingement. Of those silicon carbide materials tested, the 50 to 60 percent dense gave the best abradability in both fine and coarse grained materials. However, the former show only fair thermal stress resistance and the latter evidenced high velocity particle erosion, as stated previously.

The appearance of the low density silicon carbide samples after rub test is typified in Figures 12 and 13.

Porous, low density sintered silicon nitride samples exhibited poor abradability. The 20 percent dense samples failed before a rub pattern could develop. Because of the inherent weakness of the low density structure, it was unable to sustain the mechanical stresses imposed. The 60 percent dense sample shattered after 10 seconds of contact with the blade tip. High thermal and mechanical stresses were indicated by the instrumentation and sample appearance after test.

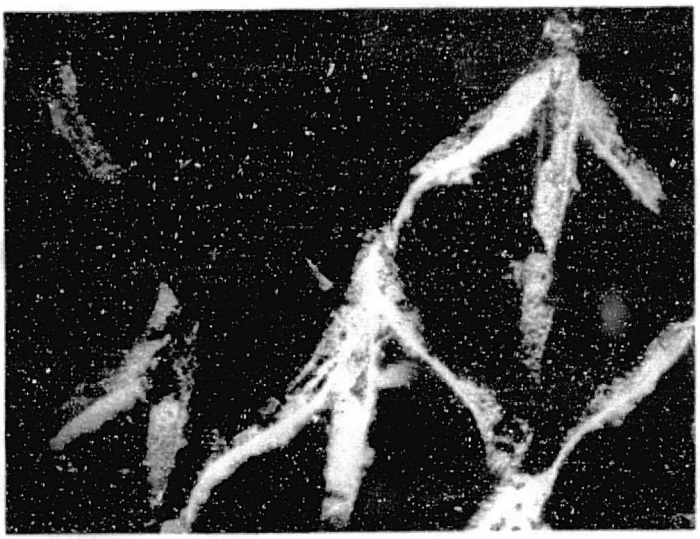

Magnification: 16X

Figure 5.

2 mm Cell Unfilled Honeycomb Silicon Nitride Before Oxidation Test

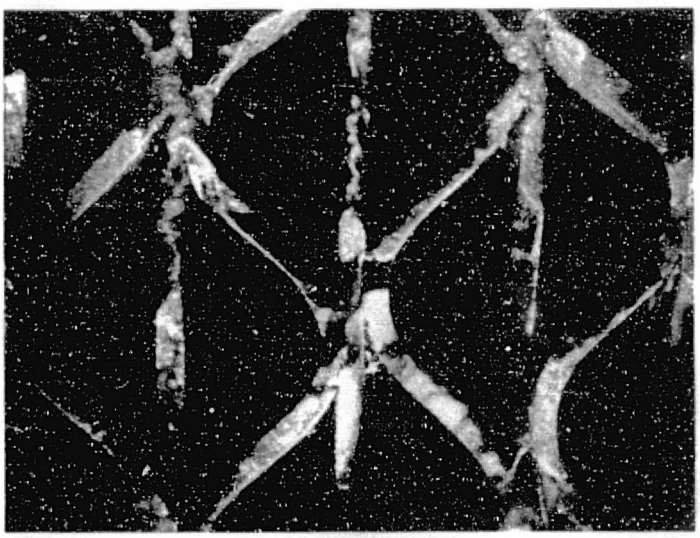

Magnification: 16X

Figure 6.

2 mm Cell Unfilled Honeycomb Silicon Nitride After 500 Hours Oxidation Test At 1370°C

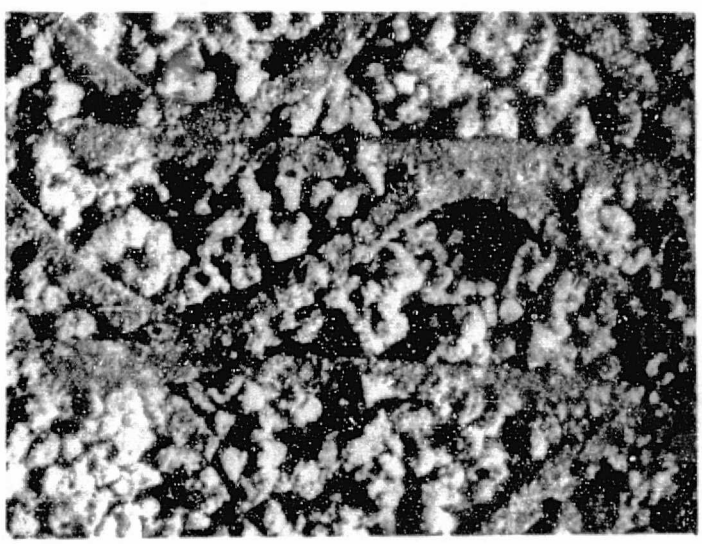

Magnification: 24X

Figure 7.

2 mm Cell Filled Honeycomb Silicon Nitride Before Oxidation Test

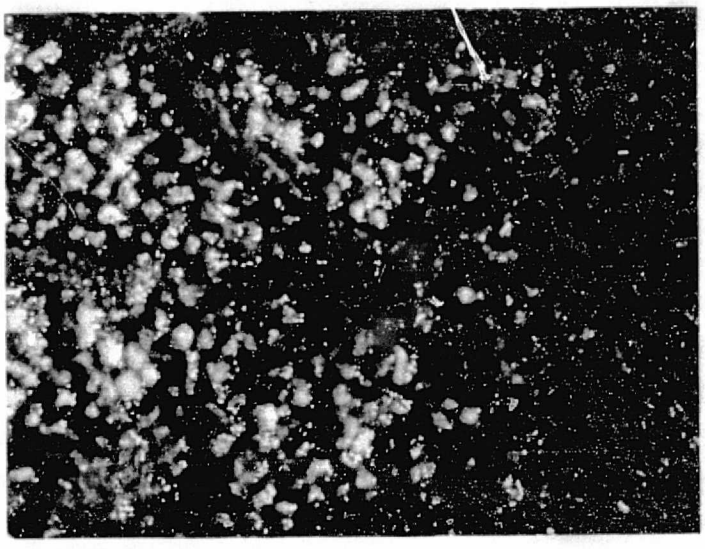

Magnification: 24X

Figure 8.

2 mm Cell Filled Honeycomb Silicon Nitride After 50 Hours Oxidation at 1370°C

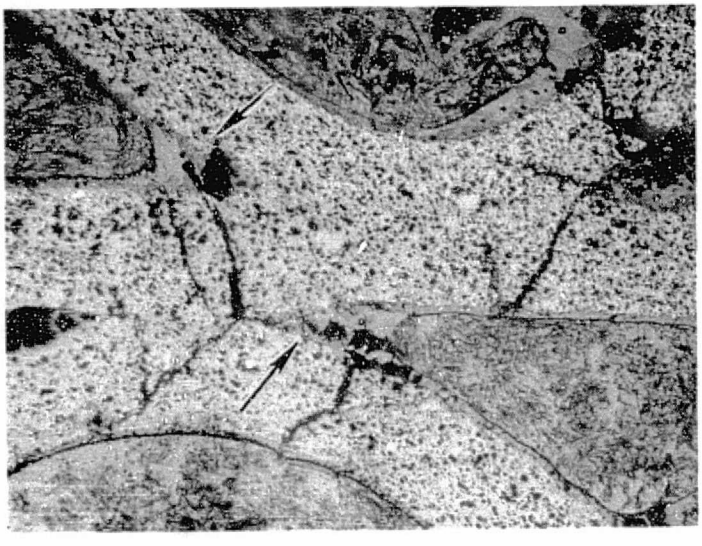

Magnification: 75X

Figure 9.

Nodal Joints of 2 mm Cell Filled Honeycomb Silicon Nitride After 500 Hours Oxidation at 1370°C

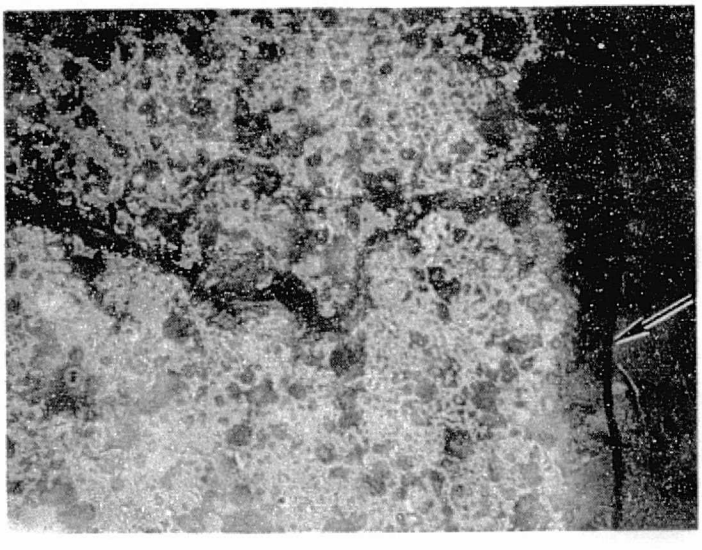

Magnification: 500X

Figure 10.

Oxide Layer Formed on 2 mm Cell Filled Honeycomb Silicon Nitride After 500 Hours Oxidation at 1370°C

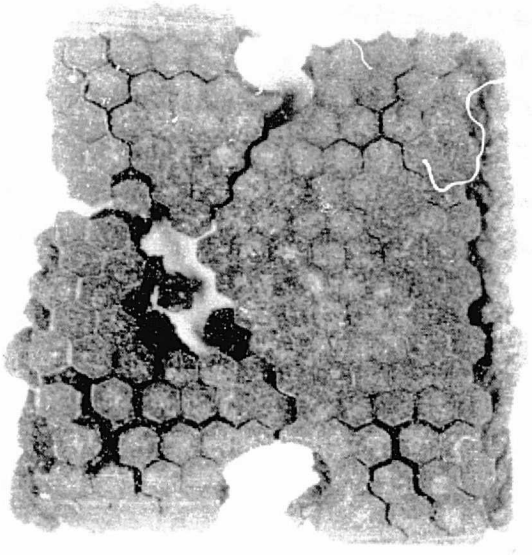

Figure 11.

Bradelloy 500 Specimen After Oxidation Test at 1370°C for 2 Hours

Reaction bonded 60 percent dense silicon nitride and sintered silicon nitride from two alternate vendors were also tested with similar results (Figs. 14 and 15). The reaction bonded structure shattered completely during test with no evidence of abrading prior to failure. Mechanical stresses and blade wear were low. High thermal stresses, due to frictional heating, were indicated by blade and sample appearance. The sintered structure also did not abrade. Cracking and chipping occurred in the rub area without total material loss. Transfer of the blade material to the ceramic surface was also evident. The sintered structure shows some improvement over reaction bonded structures, but cannot be described as a true abradable material.

Rub tests on 2 mm and 1 mm cell size honeycomb silicon nitride gave similar results (Fig. 16). Neither material showed evidence of mechanical failure during rub and blade wear was low. Honeycomb samples filled with silicon nitride powder were also tested. During rub the filler was lost and the sample then behaved like the unfilled material. No observable benefit was obtained from filling the honeycomb as originally proposed. The materials behaved in a manner similar to low density silicon nitride materials.

Ceramic tipped blades were tested and compared with a similar MAR-M421 configuration. The comparison between hot pressed silicon nitride, hot pressed silicon carbide and MAR-M421 alloy blade tips was made on 2mm cell size honeycomb nitride.

Figures 17 and 18 illustrate the appearance of a MAR-M421 turbine blade (reduced in the tip section to parallel the ceramic inserts) after rub. The tip is worn for approximately 64 percent of the total penetration. Wear is over twice that of the ceramic tips from similar tests. Views are presented in Figures 19 and 20 of silicon nitride tips subjected to this test. A single fracture has occurred. Although not readily visible, small

Table 3

Room Temperature Abradable Rub Tests

Test Number	System Number (Table 1)	Abradable Material	Blade Material	Blade Wear	Sample Temperature Rise (2)	Shear Force (Max) (3)	Shear Force (Avg.) (3)	Comments
1	Baseline	Bradelloy 500	MAR-M421	0.051 mm	55°C (100°F)	(4)	(4)	Localized backing to honeycomb failure and hard surface glaze.
2	2	Silicon Nitride 2 mm cell	MAR-M421	0.025 mm	75°C (130°F)	37 kgf (82 lbf)	14 kgf (30 lbf)	Red heat visible on contact. Blade shows heat coloration but no melting. Tip scored.
3	20	Silicon Carbide 50% dense 100/60 grit	MAR-M421	None	(4)	(4)	(4)	Sample delaminated and failed due to vibration and/or air blast prior to rub.
4	18	Silicon Carbide 40% dense 320 grit	MAR-M421	None measurable	44°C (80°F)	34 kgf (74 lbf)	6.8 kgf (15 lbf)	Scoring on leading blades, others unmarked. Wear less than can be measured.
5	10	Reaction Bonded Silicon Nitride 60% dense	MAR-M421	None measurable	(4)	23 kgf (50 lbf) Then shattered	11 kgf (25 lbf)	Sample rubbed smoothly first five seconds. At six seconds shear strain rapidly increased and sample shattered at ten seconds total time.
6	17	Silicon Carbide 320 grit 50% dense	MAR-M421	None measurable	100°C (180°F)	20 kgf (45 lbf)	13 kgf (25 lbf)	Smooth rub with some blade transfer to the abradable.
7	16	Silicon Carbide 320 grit 60% dense	MAR-M421	Slight scoring	133°C (240°F)	(4)	(4)	Intermittent contact initially due to sample fracture. Complete breakup of sample after 15 seconds.
8	22 & 25	Silicon Carbide 100/80 grit 60% dense	MAR-M421	Very light blade scoring	69°C (125°F)	3.2 kgf (7 lbf)	2.7 kgf (6 lbf)	No blade damage but structure eroded in non-contact areas in high velocity air from blade tips.
9	3	Silicon Nitride 1 mm cell	MAR-M421	No overall blade wear but scoring in nodes	92°C (165°F)	32 kgf (70 lbf)	14 kgf (30 lbf)	The test sample exhibited more blade friction than the 2 mm cell material. Light metal transfer (scabbing) also occurred.
10	Baseline	Bradelloy 500	MAR-M421	0.051 mm	133°C (240°F)	50 kgf (110 lbf)	30 kgf (65 lbf)	Red heat visible. Smeared Hastalloy core. Penetrated 0.25 mm into specimen.
11 (5)	Baseline	Bradelloy 500	MAR-M421	0.025 mm	194°C (330°F)	68 kgf (150 lbf)	23 kgf (50 lbf)	Incursion rate 0.013 mm/sec. Sample came loose during test. Heavy glaze.
12 (5)	Baseline	Bradelloy 500	MAR-M421	Grooved - Not measurable	278°C (500°F)	32 kgf (70 lbf)	27 kgf (60 lbf)	Incursion rate 0.051 mm/sec. Blade engaged evenly - red glow across surface.
13	Baseline	Bradelloy 500	MAR-M421	0.048 mm	200°C	54 kgf (120 lbf)	14 kgf (30 lbf)	Glazing produced non-uniform rub from local build-up of material.
14 (5)	Baseline	Bradelloy 500	MAR-M421	0.066 mm	167°C (300°F)	36 kgf (80 lbf)	14 kgf (30 lbf)	Penetration rate 0.013 mm/sec. Specimen eroded - blade loss high.
15	5	2 mm Silicon Nitride	HP Silicon Nitride	0.11 mm	41° C (75° F)	(6)	(6)	Ceramic tip worn. No chipping evident. Tip to seal wear is 1 to 6.
16	5	2 mm Silicon Nitride	Silicon Carbide	0.39 mm	39° C (72° F)	(6)	(6)	Numerous fractures in ceramic tip. Tip to seal wear ratio 1 to 1.
17	25	Silicon Carbide 100/60 Grit 60 % Dense	Silicon Carbide	0.19 mm	Non-Indicated	(6)	(6)	Tip fractures again evident.
18	34	Reaction Bonded Silicon Nitride	MAR-M421					Specimen Shattered on Contact
19	36	Reaction Bonded Silicon Nitride (Sintered)	MAR-M421	0.15 mm	99° C (180° F)	(6)	(6)	High Surface Heat Generation During Rub, Specimen Cracked.

Notes:
(1) Standard test conditions: Tip speed - 427 MPS; Incursion rate - 0.025 mm/sec; Interference depth - 0.76 mm
(2) Max. temperature rise during rub as indicated by a thermocouple 1.3 mm beneath initial contact area
(3) Shear force exerted on sample during test as indicated by strain gages on sample support
(4) Significant data not available due to sample failure
(5) Non-standard test. Run to find more baseline material.
(6) Force less than normal equipment sensitivity due to reduced blade tip and fracture on contact.

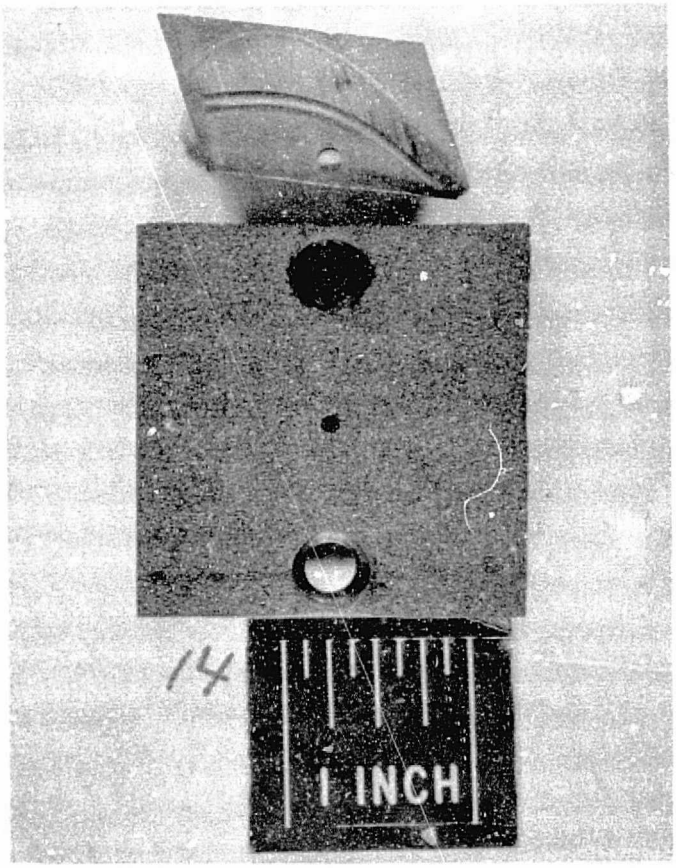

Figure 12.

Silicon Carbide, 60 Percent Dense, 100/60 Mesh, After Rub Testing

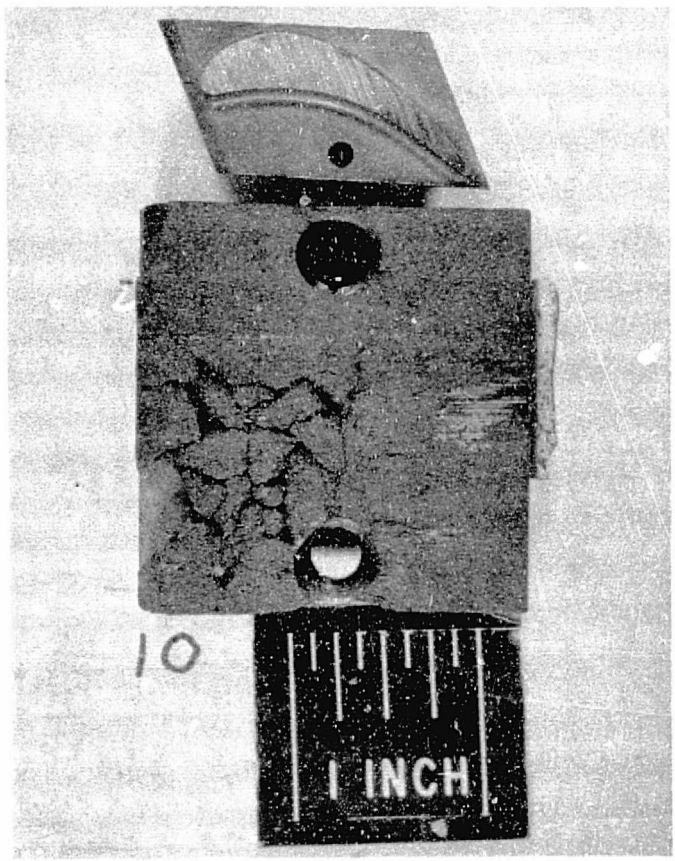

Figure 13.

Silicon Carbide, 50 Percent Dense, 320 Mesh, After Rub Test

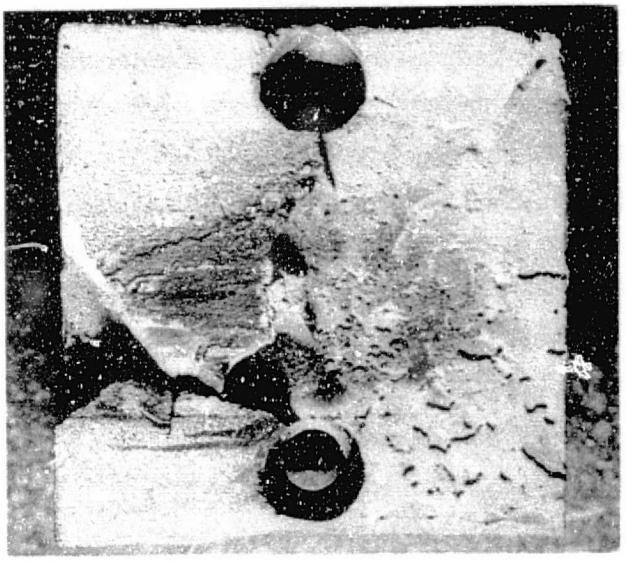

Figure 14.

Reaction Bonded, 60 Percent Dense,
Silicon Nitride After Rub Test

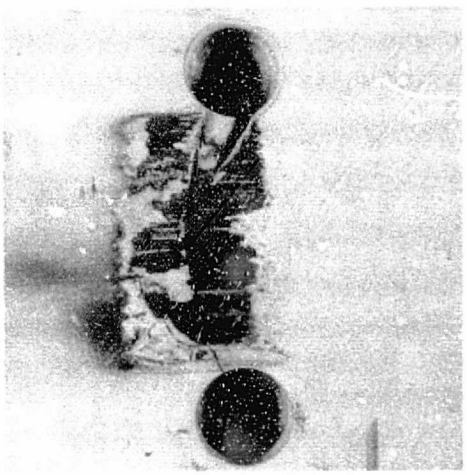

Figure 15.

Sintered, 60 Percent Dense,
Silicon Nitride After Rub Test

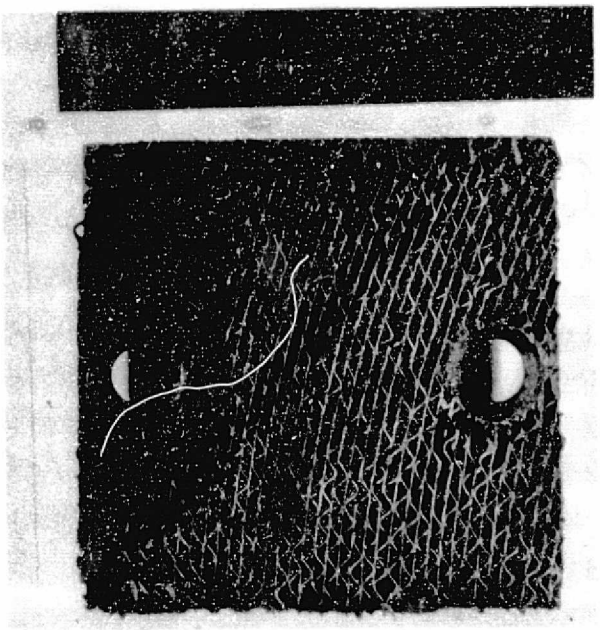

Figure 16.

2 mm Honeycomb Silicon Nitride
After Rub Test

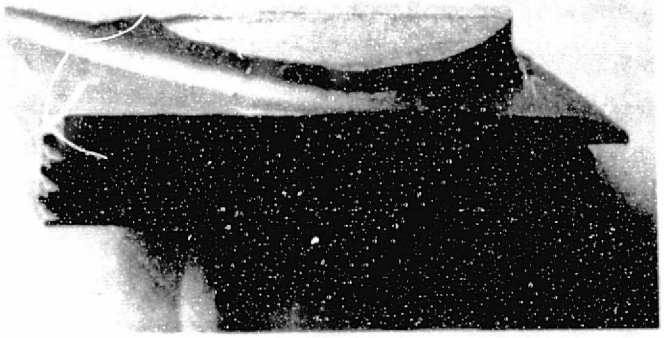

Figure 17.

MAR-M421 Blade Tip After Test
Rub on Silicon Nitride Honeycomb

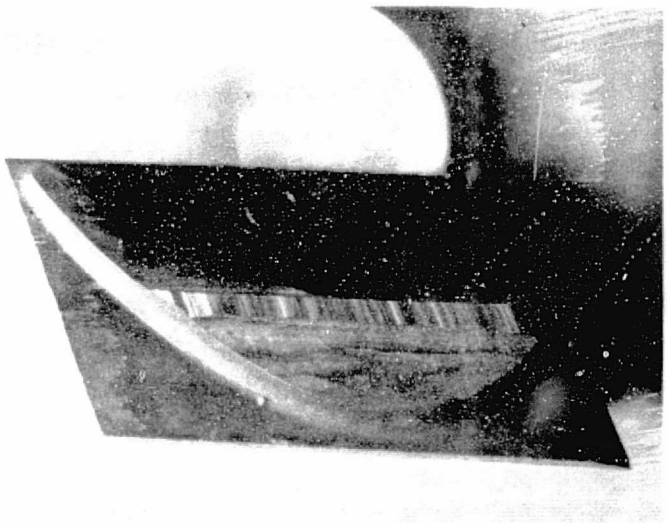

Figure 18.

End View of MAR-M421 Blade After Rub Test

Magnification: 2.75X

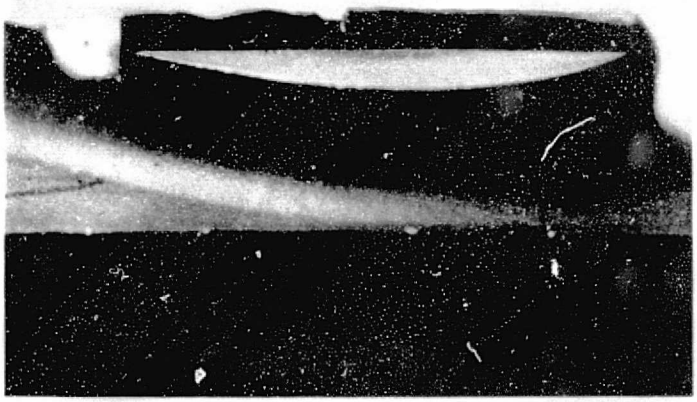

Figure 19.

Silicon Nitride Blade Tip Profile After Rub Test

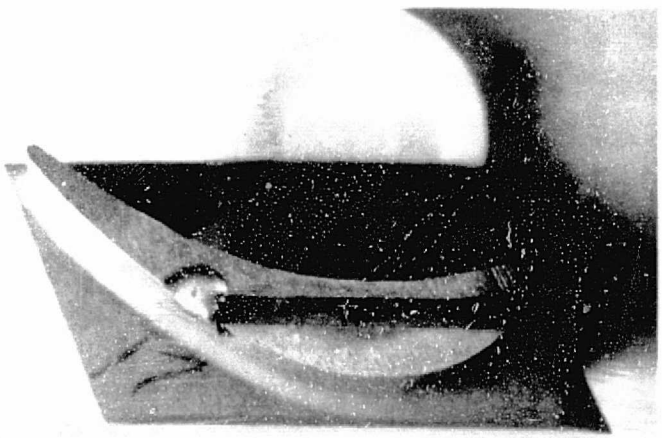

Magnification: 1.5X

Figure 20.

Silicon Nitride Blade Tip After Rub Test

irregularities exist in the dovetail creating point contact in some regions. Very little edge chipping has occurred and the overall wear resembles a metal rather than a brittle ceramic material. The tip to seal wear is approximately one to six in contrast to the two-to-one ratio of the metal tip.

Identical rub tests were also conducted with silicon carbide blade tips, as shown in Figures 21 and 22. Again, a single cross sectional fracture of the tips occurred during rub. Wear on this tip differed considerably from those previously tested. The tip wear was exceedingly irregular. Numerous fractures occurred during rub with the subsequent loss of blade tip particles rather than the comparatively uniform continuous wear exhibited by the metal and silicon nitride tips. This tendency to fracture rather than wear is clearly evident in Figure 23, which is a higher magnification of the silicon carbide blade edge. The local fracture planes and tendency to chip during rub is evident. Tip to seal wear ratio is approximately one to one, which is half that of the metal blade but six times the wear of the silicon nitride tip under similar test conditions.

The silicon carbide blade tips, after rub on a silicon carbide abradable structure, are illustrated in Figures 24 and 25. The edge fracture previously observed when this tip was tested against the silicon nitride structure is evident. Tip wear against the low density silicon carbide was about half the wear obtained when this tip material was tested on a silicon nitride structure as previously reported.

During the program glass and metal bonds were used to join the abradable to a backing. Both demonstrated the ability to wet the ceramics and produce a strong joint. However, the metal alloy used for joining did not accommodate the stresses generated during thermal cycling. The glass bond was less susceptible to failure and this method was used to fabricate samples for abradability testing at 1370°C. Abradability testing of ceramics bonded to a ceramic backing were unsuccessful due to bond failure. The backing to abradable bond failed during test. Testing of the composite system was postponed for lack of a reliable joining method.

Silicon nitride honeycomb was rub tested at 1370°C. The sample was mechanically retained using spring loaded clamps to compensate for thermal expansion differentials between the core and the holder. During test, the sample delaminated along nodal bonds to produce independent sections three to six cells wide for the full sample length. These sections rose to varying heights during test, making wear data inconsistent.

Independent bonding of each cell to the backing is required. However, in spite of this problem none of the core was destroyed during the test and little blade wear was evident. Appearance of the core surface was uniform with no evidence of failure due to rub even though some portions showed wear well in excess of the planned 0.76 mm, due to the previously noted rise of the honeycomb core.

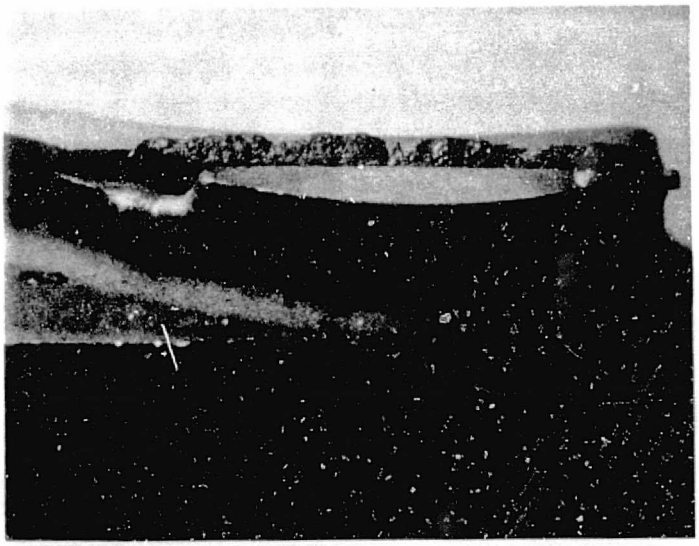

Magnification: 3X

Figure 21.

Silicon Carbide Blade Tip
After Rub Test

Figure 22.

Silicon Carbide Blade Tip
After Rub Test

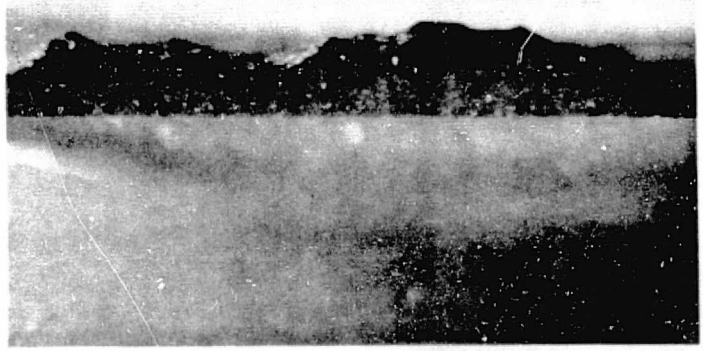

Magnification: 3X

Figure 23.

Typical Section of a Silicon
Carbide Blade Tip After Test

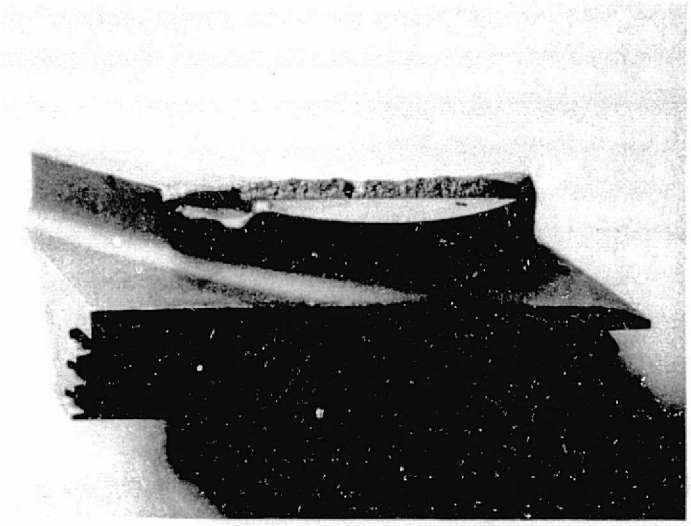

Figure 24.

Silicon Carbide Tip Profile After Rub on 60/100 Mesh Silicon Carbide, 60 Percent Dense

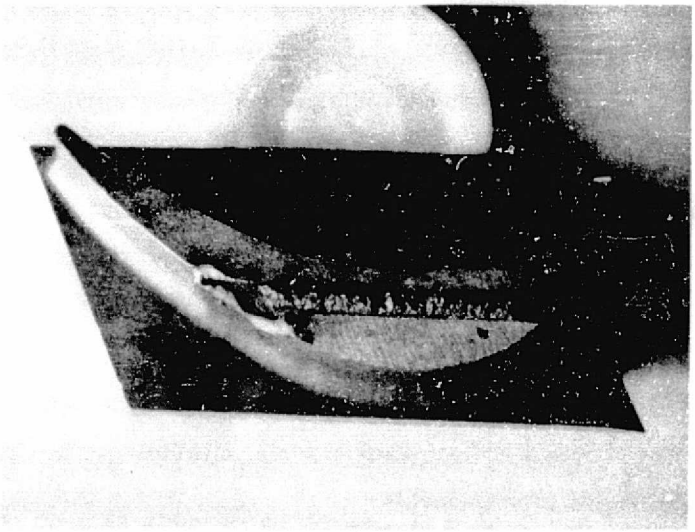

Figure 25.

Silicon Carbide Tip After Rub on 60/100 Mesh Silicon Carbide, 60 Percent Dense

As previously mentioned, Bradelloy 500 was proposed as a baseline material for the screening tests. Considerable difficulty has been encountered in establishing relevant baseline data on the Bradelloy 500 material. Under the standard test conditions the material glazed, giving a hard wear resistant surface and extremely high vibration levels in the test facility. Two test variations were tried with this material to further explain its behavior. These consisted of reducing penetration rate to half the standard value (0.012mm/sec) and in a second test the rate was doubled (0.050mm/ sec). Results of these tests are reported as tests 12, 13, and 14 in Table 3 and are shown in Figures 26, 27 and 28. Increasing the penetration rate increased the sample temperature rate of rise. Shear force was uniform during this test and the high stress peaks encountered at the lower feed rates were eliminated. After test the sample was free of the glazing effects observed in the tests at lower penetration rates.

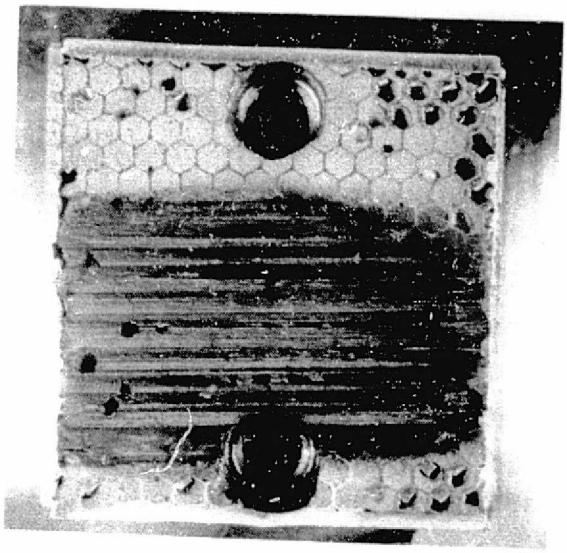

Figure 26.

Bradelloy Penetration Rate,
0.050 mm/sec

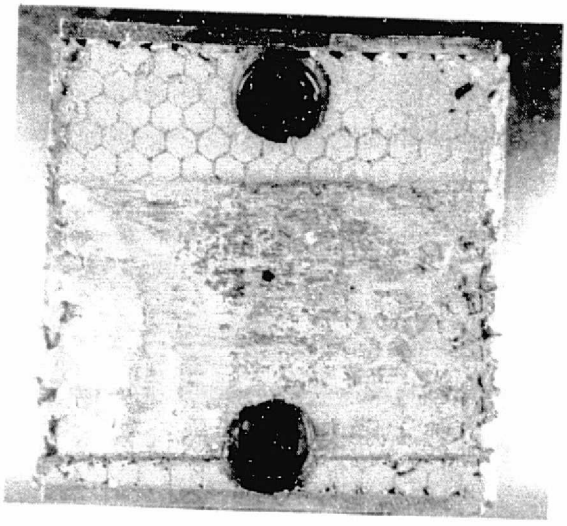

Figure 27.

Bradelloy Penetration Rate,
0.025 mm/sec

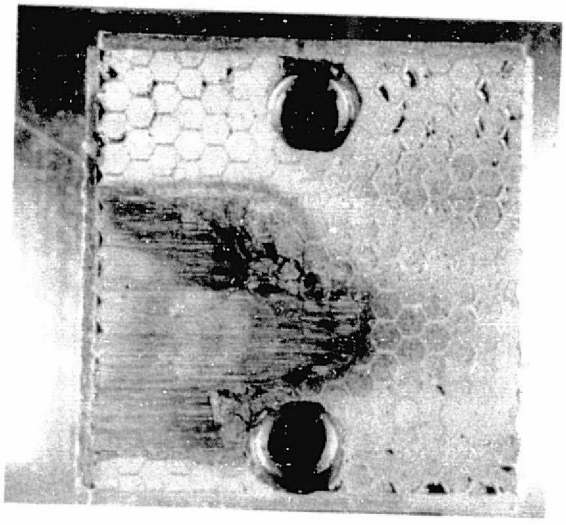

Figure 28.

Bradelloy Penetration Rate,
0.012 mm/sec

2.2.4 Ballistic Impact Test

Ballistic impact testing for all samples was performed using the following test conditions:

Impingement angle	30 degrees
Velocity	127 mps
Projectile diameter	4.78 mm
Projectile weight	0.440 grams

After impact, samples were compared with respect to size of the impact damaged area, depth of projectile penetration, presence of surface cracking and general loss of physical integrity (Table 4). Figures 29 through 35 are representative of the results of these tests. Low density silicon nitride and silicon carbide materials exhibited the most damage. Areas with deep projectile penetration and surface cracking are evident in Figure 29. The silicon carbide sample in Figure 30 also shows large material losses in the area of impact. Damage done to the higher density silicon nitride and silicon carbide materials in Figures 31 and 32 is significantly less. However, surface cracking still exists.

Unfilled corrugated silicon nitride structures performed well during impact testing (Figs. 33-35). The corrugated structures tended to isolate the effects of impact. Unfilled samples showed no sign of crack propagation. The effect of impact was localized. Penetration depths were greater than those in solid silicon nitride and silicon carbide samples. Filled honeycomb silicon nitride samples exhibited cracking through the thickness of the ribbon. The cracking was also transmitted to adjacent areas by the filler in a manner similar to solid samples previously described.

2.2.5 Hot Gas Erosion Testing

Gas erosion tests were performed on filled and unfilled 1 mm cell silicon nitride and on reaction bonded silicon nitride (Figs. 36 thru 41). Filler material was a mixture of silicon nitride powder and a silica glass. Test duration was 100 hours with a temperature of 1370°C at the sample surface. All samples were cooled to room temperature every 24 hours for inspection and weighing.

During the erosion test the filled structure suffered an almost complete loss of the filler material (Fig. 37). The glass component of the filler was separated from the ceramic powder component at the high temperature and flowed towards the honeycomb surface. The ceramic powder component was then carried away by the high velocity gases. A similar behavior was reported for static oxidation tests. In the latter, the glass (with ceramic particles intermixed) reached the surface where it remained as a glassy deposit in the absence of high velocity gases. The glassy deposit was not analyzed.

Table 4

Ballistic Impact Test Results at Ambient Temperature (Velocity 127 mps, Impingement Angle 30 Degrees, 4.78 mm Steel Spheres)

			Damaged Area			
Test Series	System	Material	Length (mm)	Width (mm)	Depth (mm)	Comments
1	2	Corrugated Si_3N_4 2 mm cell size	30.5	8.9	6.4	Uniform crater ending abruptly as energy dissipated
2	3	Corrugated Si_3N 1 mm cell size	22.9	8.9	5.1	See above Test 1
3	10 & 13	Reaction bonded Si_3N_4 - 60° dense	*	*	*	No penetration, crack in sample at point of impact
4	12 & 15	Reaction bonded Si_3N_4 - 20% dense	11.4	4.4	2.5	Shallow crater with minor edge spalling
5	16	Silicon carbide 60% dense	**	**	**	Specimen shattered on impact
6	17	Silicon carbide 50% dense	6.4	3.2	1.3	Slight crack originating at impact area
7	18	Silicon carbide 40% dense	11.4	3.4	2.5	No crack formation. Penetration deeper than for silicon nitride
8	22 & 25	100/60 silicon carbide 60% dense	6.4	3.8	2.5	Deep short crater
9	23 & 26	100/60 silicon carbide 50% dense	16.5	6.4	5.1	Crater size approximately twice that of 60% dense material
10	24 & 27	100/60 silicon carbide 40% dense	**	**	**	Specimen delaminated upon impact
11	4	Filled corrugated silicon nitride 2 mm cell size	17.1	8.4	9.8	See test 1
12	5	Filled corrugated silicon nitride 1 mm cell size	10.5	7.2	5.1	See test 1
13	34	Reaction bonded silicon nitride 60% dense	*	*	*	No penetration, cracks in sample at points of impact
14	36	Sintered silicon nitride, 60% dense	**	**	**	Sample shattered. Cracks propagating from impact area

* Specimen showed no measurable loss.

** Specimen destroyed on impact.

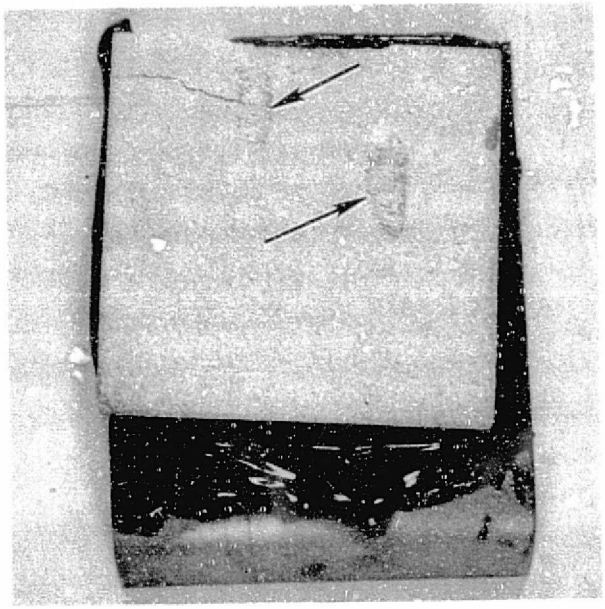

Figure 29.

Silicon Nitride 40 Percent Dense
After Impact Test
(Arrows Indicate
Impact Area)

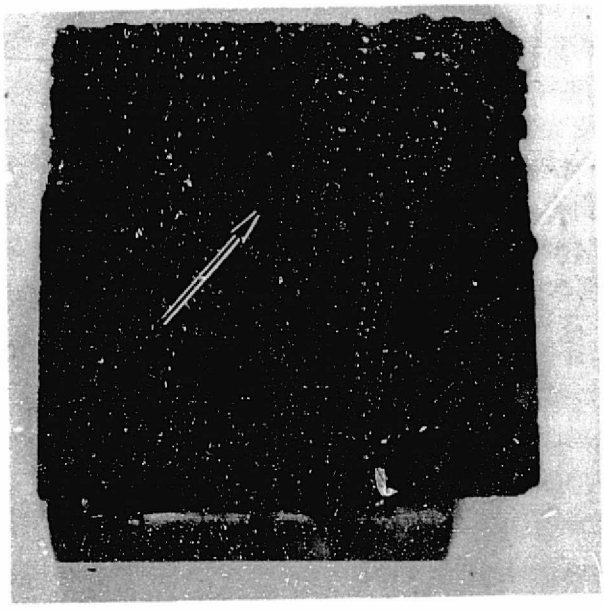

Figure 30.

Silicon Carbide 40 Percent Dense
After Impact Test
(Arrows Indicate
Impact Damage)

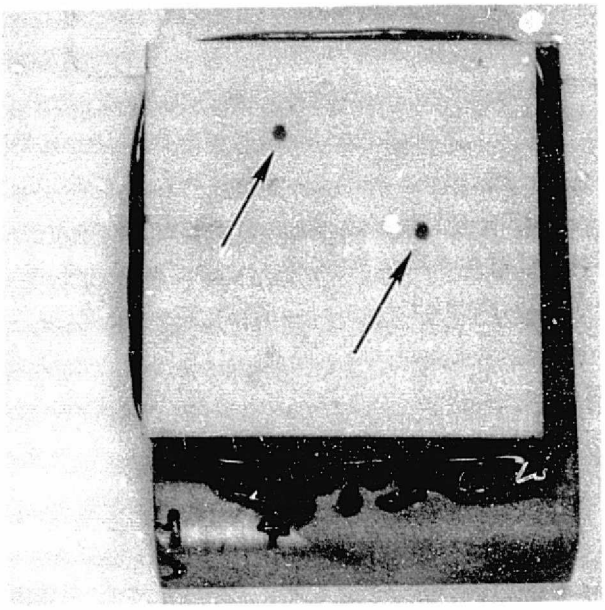

Figure 31.

Silicon Nitride 60 Percent Dense
After Impact Test
(Arrows Indicate
Impact Area)

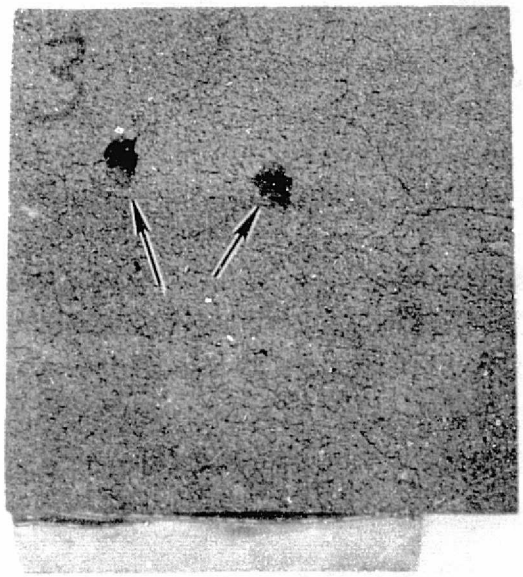

Figure 32.

Silicon Carbide 60 Percent Dense
After Impact Test
(Arrows Indicate
Impact Area)

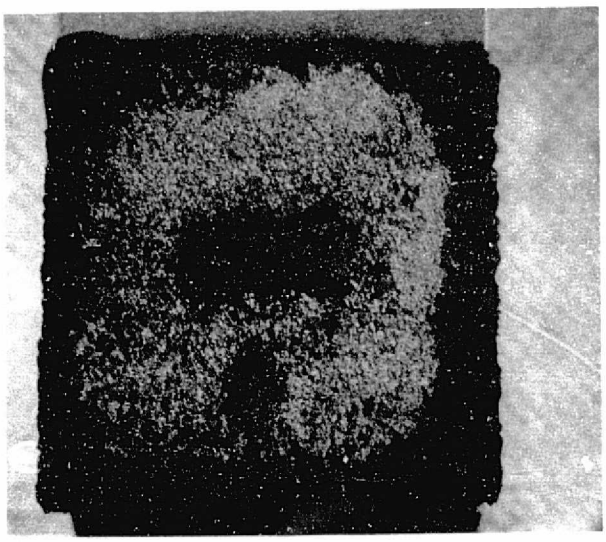

Figure 33.

Filled 1 mm Cell Silicon Nitride After Impact

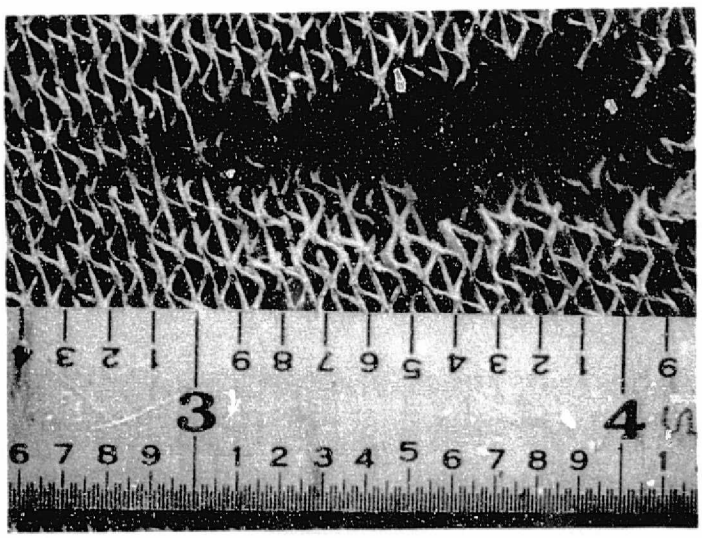

Figure 34.

Unfilled 2 mm Honeycomb Silicon Nitride After Impact Test

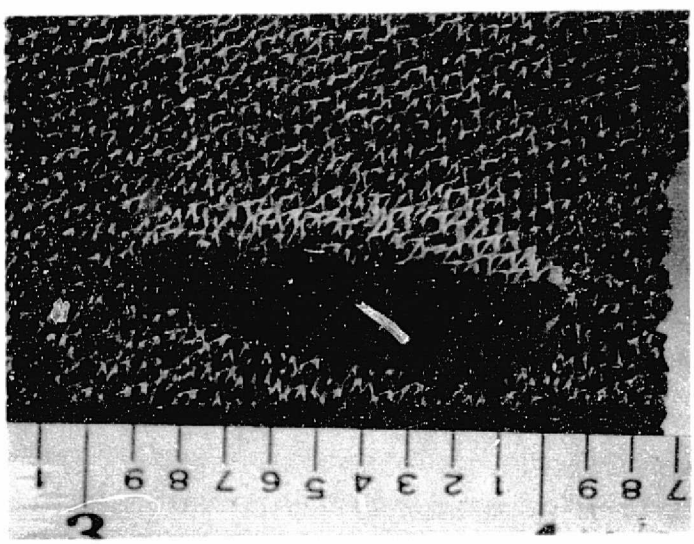

Figure 35.

Unfilled 1 mm Honeycomb Silicon Nitride After Impact Test

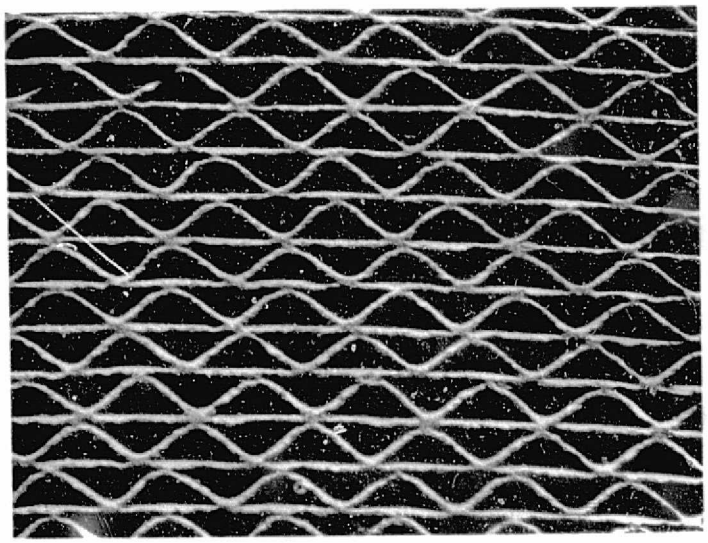

Magnification: 9.5X

Figure 36.

1 mm Cell Unfilled Honeycomb Silicon Nitride Before Erosion Test

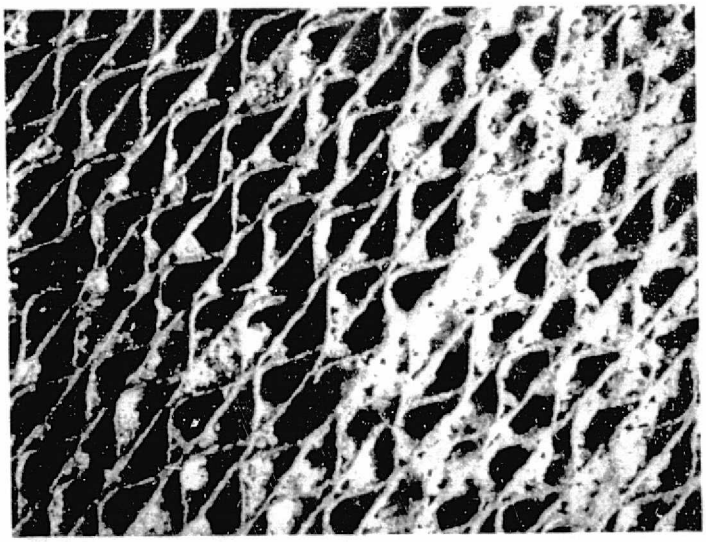

Magnification: 9.5X

Figure 37.

1 mm Cell Filled Honeycomb Silicon Nitride After 100 Hours Hot Gas Erosion

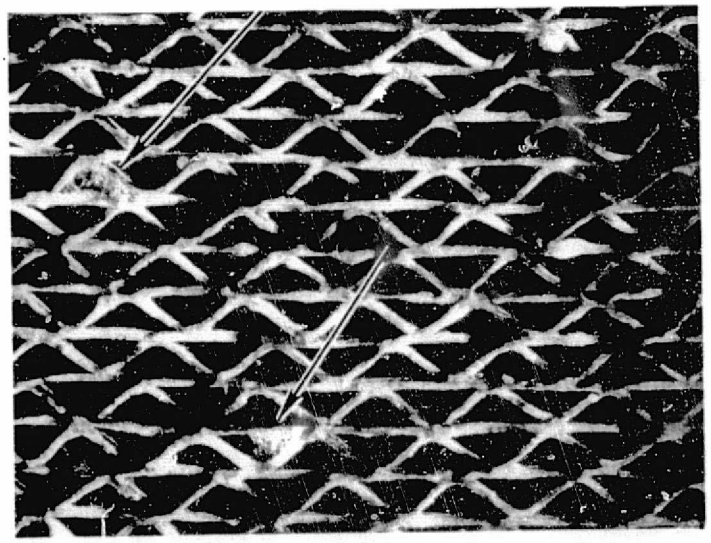

Magnification: 9.5X

Figure 38.

1 mm Cell Unfilled Honeycomb Silicon Nitride After 100 Hours Hot Gas Erosion (Arrows Indicate Exuded Glassy Phase)

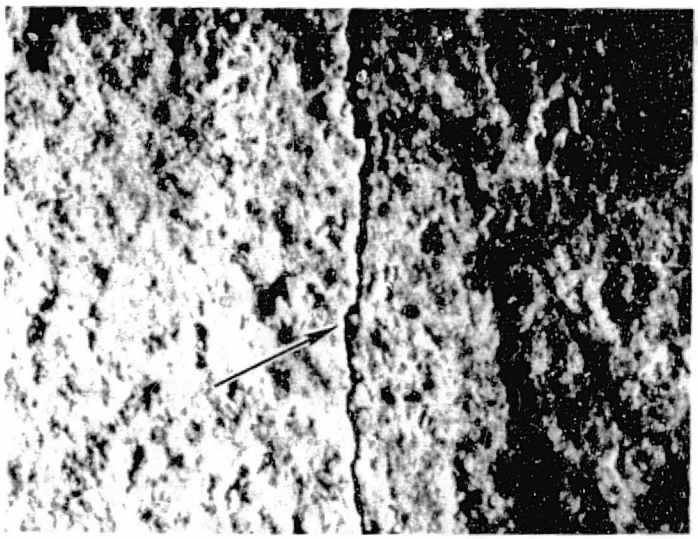

Magnification: 22X

Figure 39.

Reaction Bonded Silicon Nitride After Hot Gas Erosion Test Showing Cracking Due to Particle Impact

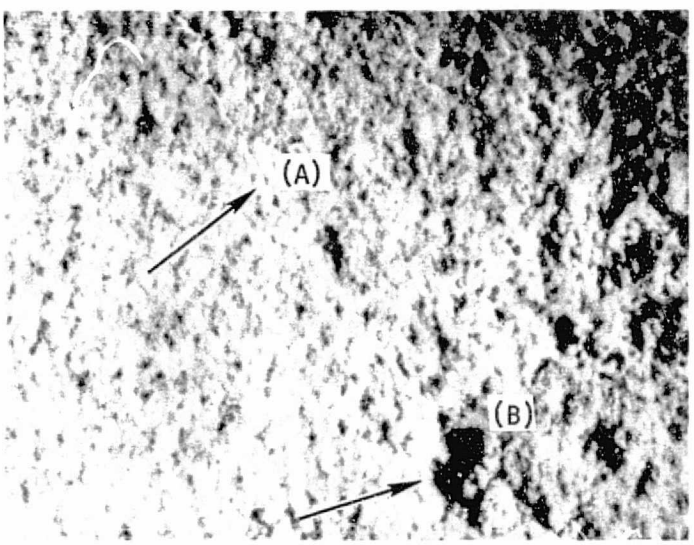

Magnification: 22X

Figure 40.

Reaction Bonded Silicon Nitride After Hot Gas Erosion Test Showing Crack Propagation (A) From Impact Crater (B)

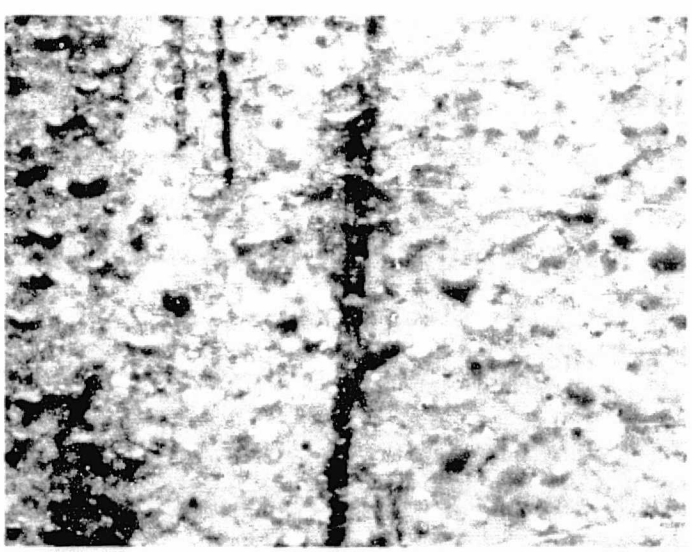

Magnification: 22X

Figure 41.

Reaction Bonded Silicon Nitride After Hot Gas Erosion Showing Glassy Phase On Surface

Visual examination of the unfilled silicon nitride structure after 100 hours revealed the presence of a clear, glassy phase adhering to the cell inner walls (Fig. 38). This deposit resembles that observed in the tests of the filled structure and oxidation tests of low density materials based on silicon nitride.

Rounding and chipping of the ribbon edges were also observed during erosion testing of the honeycomb sample. Blackish deposits on the ribbon surfaces resemble carbon particle impact. The test facility has been modified to eliminate carbon particles as a possible factor in future tests.

The surface of the reaction bonded silicon nitride material showed considerable pitting and coarsening after testing. A crater of diameter 0.91 mm can be identified as the origin of a hairline crack which extends through the full thickness of the sample (Figs. 39 and 40). The effect was not localized as with the honeycomb silicon nitride structure. A glassy phase was also present on the surface of the reaction bonded sample.

In the three material systems, weight gains were recorded rather than weight loss.

2.3 CONCLUSIONS AND RECOMMENDATIONS

After reviewing the results of Task I of the original contract it was concluded that the scope of the program should be broadened to include an optimization of silicon carbide abradables, an analytical study of ceramic blade tip inserts, a parametric study of silicon nitride rub variables and a joining study. This decision was prompted by:

1. The dependence of silicon carbide material performance on density and grain size, and the limited variations tested,
2. The success of rub tests using hot pressed silicon nitride blade tip inserts,
3. The excellent performance of silicon nitride honeycomb structures in abradability, oxidation, erosion and ballistic impact tests,
4. The difficulties encountered during Task I in bonding the ceramic abradable seal to a backing and the importance of successfully joining a highly rub tolerant seal to a high strength backing in producing a practical system.

From the cumulative data obtained from the original program, initial conclusions were drawn regarding silicon carbide abradables. The density should lie in the 60 percent range and the grain size should be a combination of fines (about -200 mesh) to enhance strength, and coarse (approximately 100 mesh) to enhance abradability and oxidation resistance while still remaining sufficiently fine to avoid high velocity particle erosion observed in previous testing.

To fully characterize a honeycomb type silicon nitride as an abradable seal material, the effect of changing rub parameters must be evaluated. Table 5 illustrates a typical set of variables that should be investigated. Rub may occur during nearly any portion of the operating regime and a single test will not characterize the material throughout this spectrum.

The great disparity between metal and ceramic expansion coefficients necessitates the development of techniques for joining a seal material to a high density, high strength ceramic backing that can be mechanically held in the metal shroud. Engine conditions dictate the need for a seal to backing bonding medium which combines thermal shock resistance with high temperature strength and long service life. The following is a list of some techniques to be considered:

- Bonding with glass interlayers
- Brazing with a modified silicon alloy
- Bonding by reaction of a silicon alloy with nitrogen
- Modified, commercially available, high temperature ceramic adhesives

Successful utilization of ceramic blade tip inserts will require a complete design analysis. This analysis will require:

- Design optimization to maintain aerodynamic efficiency of the blade
- Mechanical retention of the tip insert
- Minimizing tip fracture resulting from mechanical, thermal and vibratory stresses
- Producibility of the insert and attachment.

Table 5

Test Parameters for Abradability Tests

TIP VELOCITIES
* 427 m/sec (1400 ft/sec)
305 m/sec (1000 ft/sec)
183 m/sec (600 ft/sec)
TEMPERATURE
1370°C (2500°F)
982°C (1800°F)
538°C (1000°F)
INCURSION RATES
0.13 mm/sec (0.005 in./sec)
* 0.025 mm/sec (0.001 in./sec)
0.0051 mm/sec (.0002 in./sec)
ABRADABLE CELL SIZE
1.0 mm (0.04 in.)
2.0 mm (0.08 in.)
INCURSION DEPTH
*0.76 mm (0.03 in.)
1.5 mm (0.06 in.)

*Standard Test Conditions

APPENDIX A

BALLISTIC IMPACT TESTING EQUIPMENT

APPENDIX A

BALLISTIC IMPACT TESTING EQUIPMENT

The ballistic impact apparatus, shown in Figure 42, consists of a Crosman 0.22 caliber air rifle modified to accept precise charging with high pressure air or nitrogen gas prior to each firing. Spherical steel balls were used as the projectiles. Calibration of the rifle for pellet velocity as a function of gas pressure in the rifle is accomplished by means of a commercial ballistic chronograph.

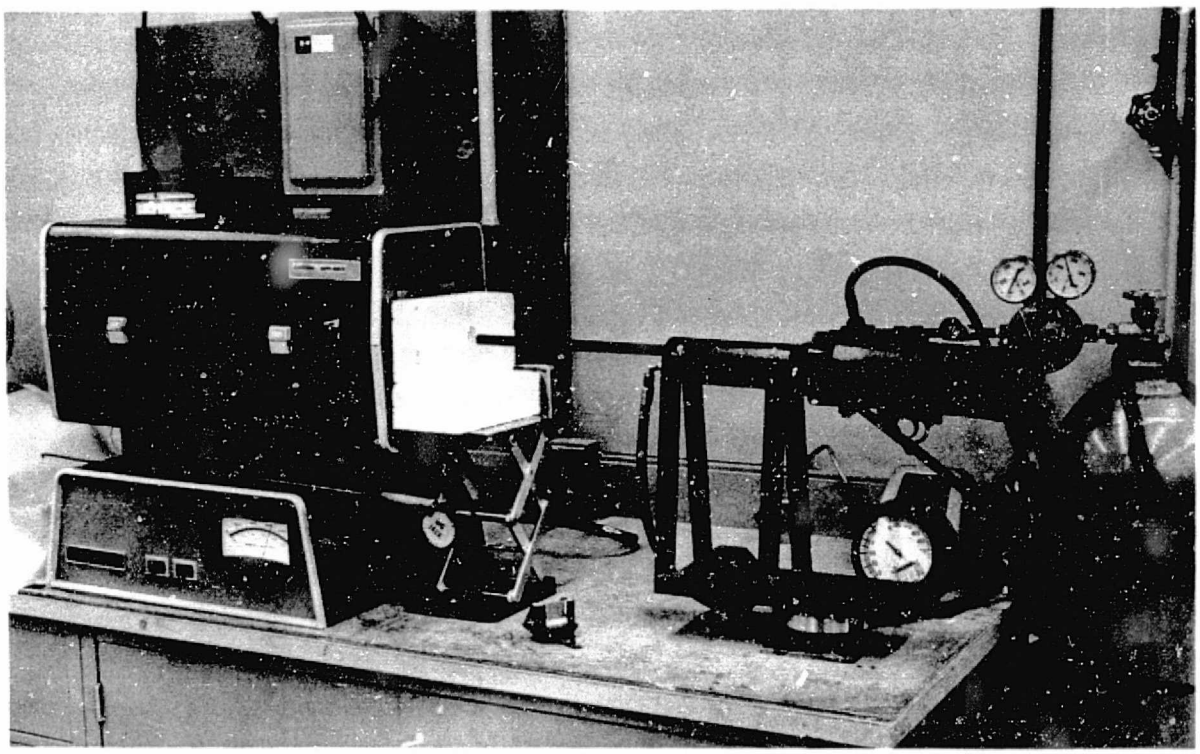

Figure 42. Typical Laboratory Setup for Impacting Ceramic Specimens

PRECEDING PAGE BLANK NOT FILMED

APPENDIX B

ABRADABILITY TESTING RIG

APPENDIX B

ABRADABILITY TESTING RIG

All abradability tests, room temperature screening and 1370°C hot tests were performed using the existing Solar seal test facility. The test rig, illustrated in Figure 43, is powered by an air driven turbine adapted for this application from one of Solar's standard production engines. Air to drive the turbine is supplied at a pressure of 0.07 Kgf/mm^2 with a mass flow of 1.4 Kgs/sec. The turbine is directly coupled to the output shaft through a flexible coupling. Abradable tip seal materials are tested at speeds of up to 427 mps and test temperatures to 1370°C. Figure 44 shows the 356 mm diameter A-286 alloy turbine disc broached with six MAR-M421 alloy turbine blades. This setup is shown for room temperature testing.

The seal material under evaluation is located immediately below this wheel (Fig. 45) on a platform advanced by a variable speed motor. The platform and seal material are instrumented with strain gages and thermocouples to obtain force and temperature data for each test.

The rig setup in Figure 46 is used for elevated temperature tests. For high temperature tests (a honeycomb tip seal is shown), the setup includes the addition of oxygem-MAPP gas torches to heat the seal material to the test temperature and shielding to reduce heatup of the wheel and bearing housing. The disc and blades are heated only when they pass through the flame, or approximately for 10 percent of the time that the seal material is heated. This provides good simulation for the air-cooled blade temperature with respect to an uncooled seal, without the complexity introduced by air cooling.

A sample configuration is shown in Figure 47. This sample is radiused to match the blade tip diameter. The simple configuration was selected to allow evaluation of a large number of materials at a reasonable cost.

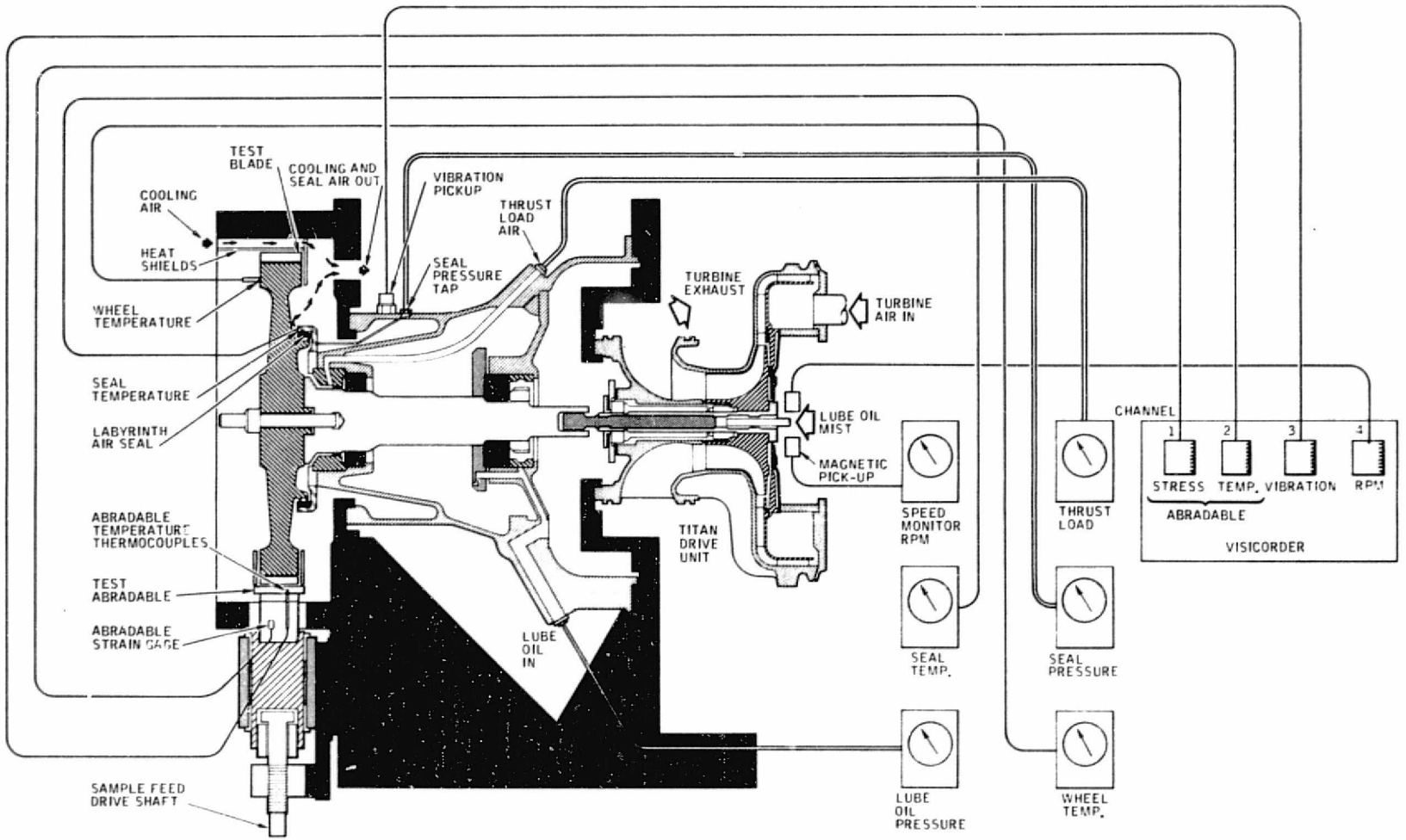

Figure 43. Schematic of Seal Test Rig

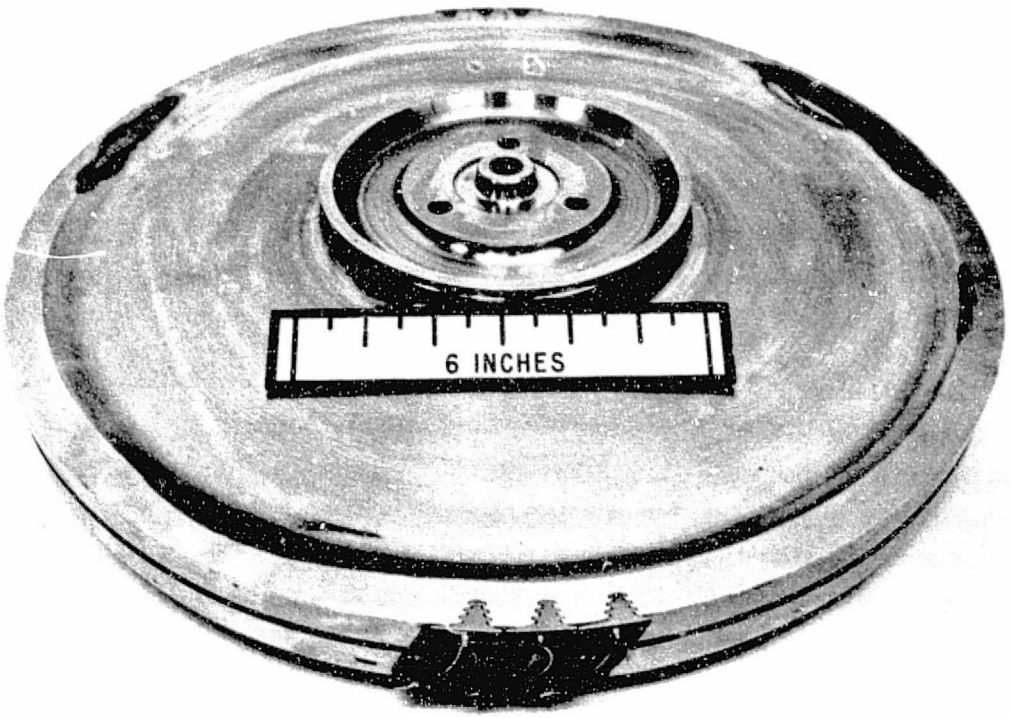

Figure 44. Seal Test Rig Wheel Showing MAR-M421 Alloy Stub Blades

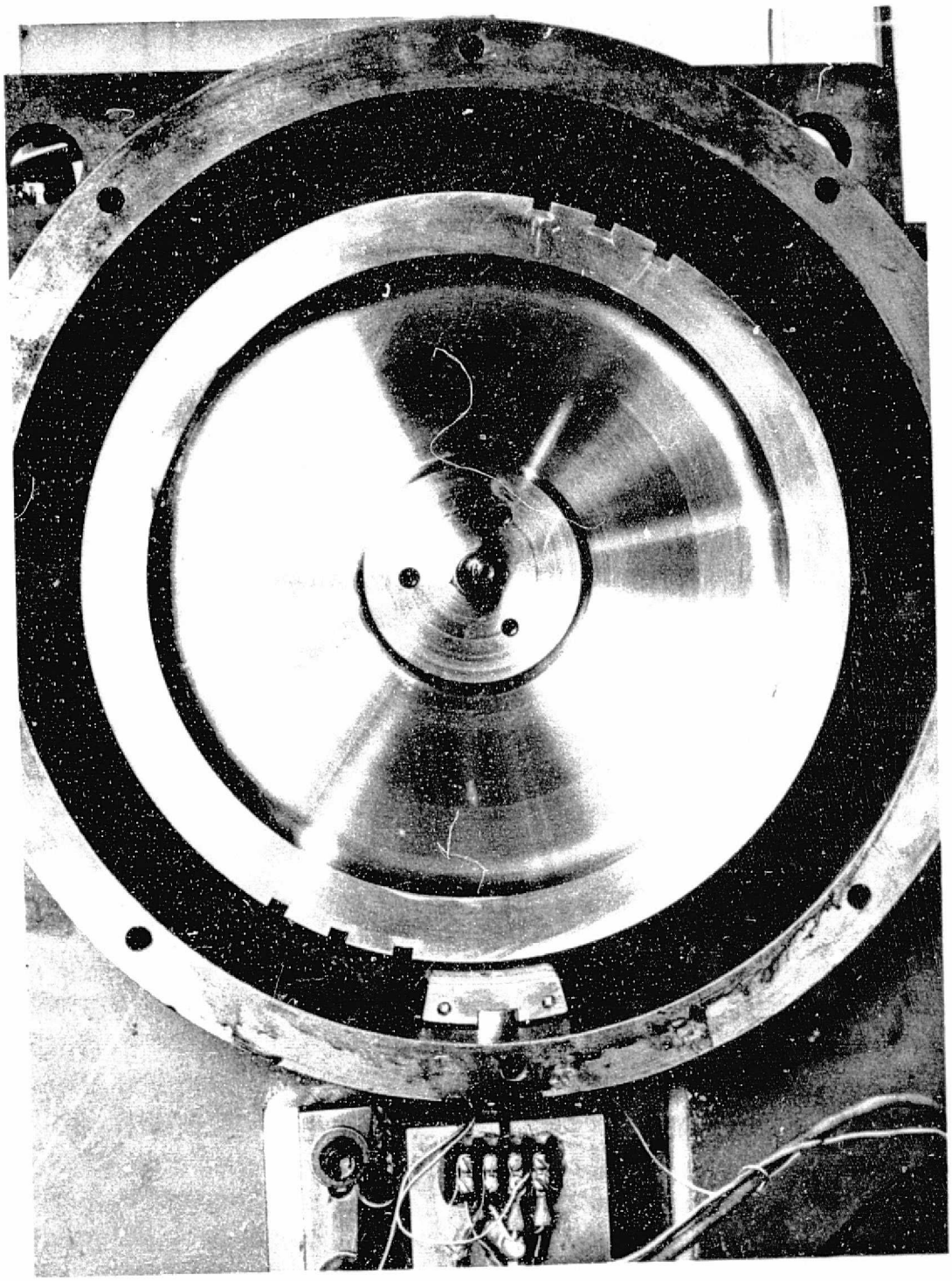

Figure 45. Seal Test Rig Showing Location of Test Seal Material

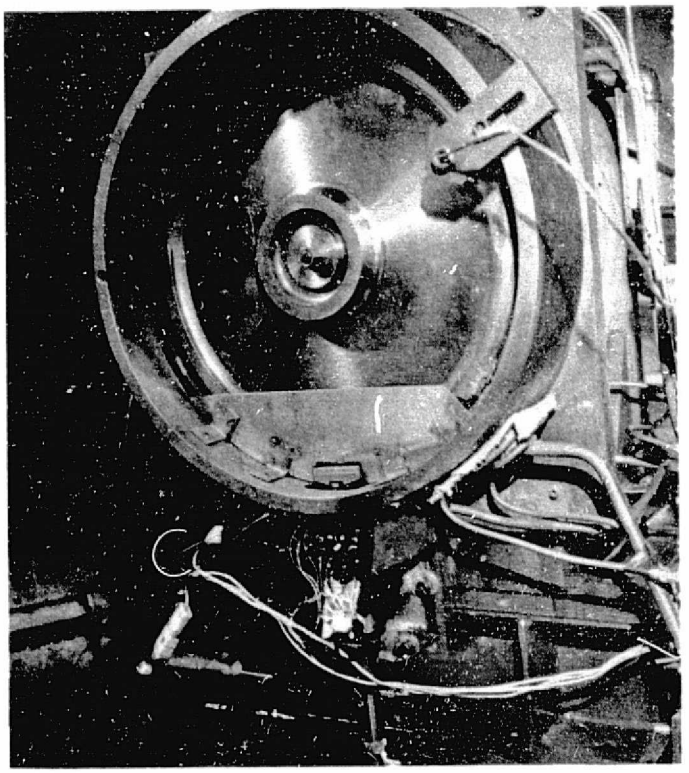

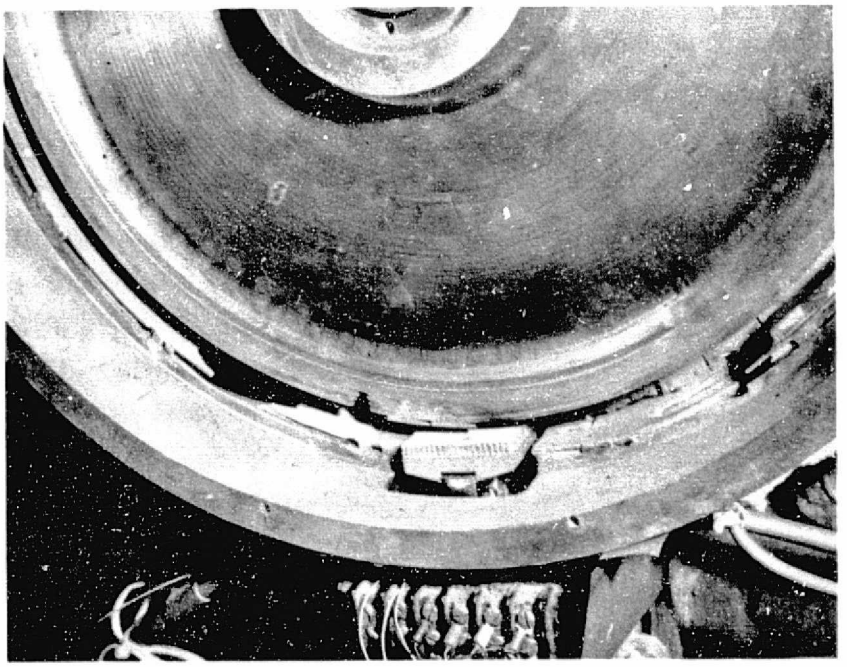

Figure 46. Seal Test Rig Showing Setup for Testing Honeycomb Blade Tip Seals at Elevated Temperature

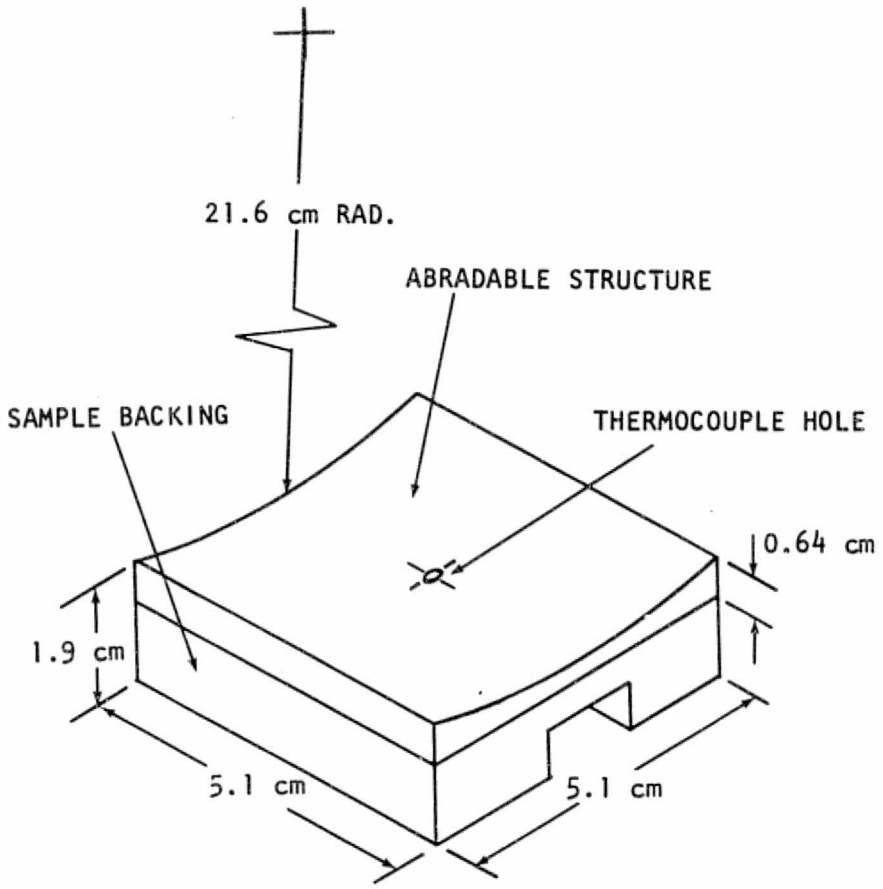

Figure 47. Typical Abradable Seal Sample

APPENDIX C

OXIDATION/EROSION RIG

APPENDIX C

OXIDATION/EROSION RIG

Solar has developed several generations of turbine environment simulators for the evaluation of materials without the expense of using a test engine. The rig used in this program includes a high-temperature combustion chamber (fabricated from Hastelloy X) burning kerosene, a nozzle and a sample holder. It is shown in Figure 48. The sample (50 mm x 50 mm x 5 mm) is held in the gas stream on a water-cooled platform. Surface temperature of the sample is maintained at 1370°C as measured optically during test. Visual observations are made periodically for sample integrity and proper operation. Test duration was 100 hours with sample removed for examination at 24-hour intervals.

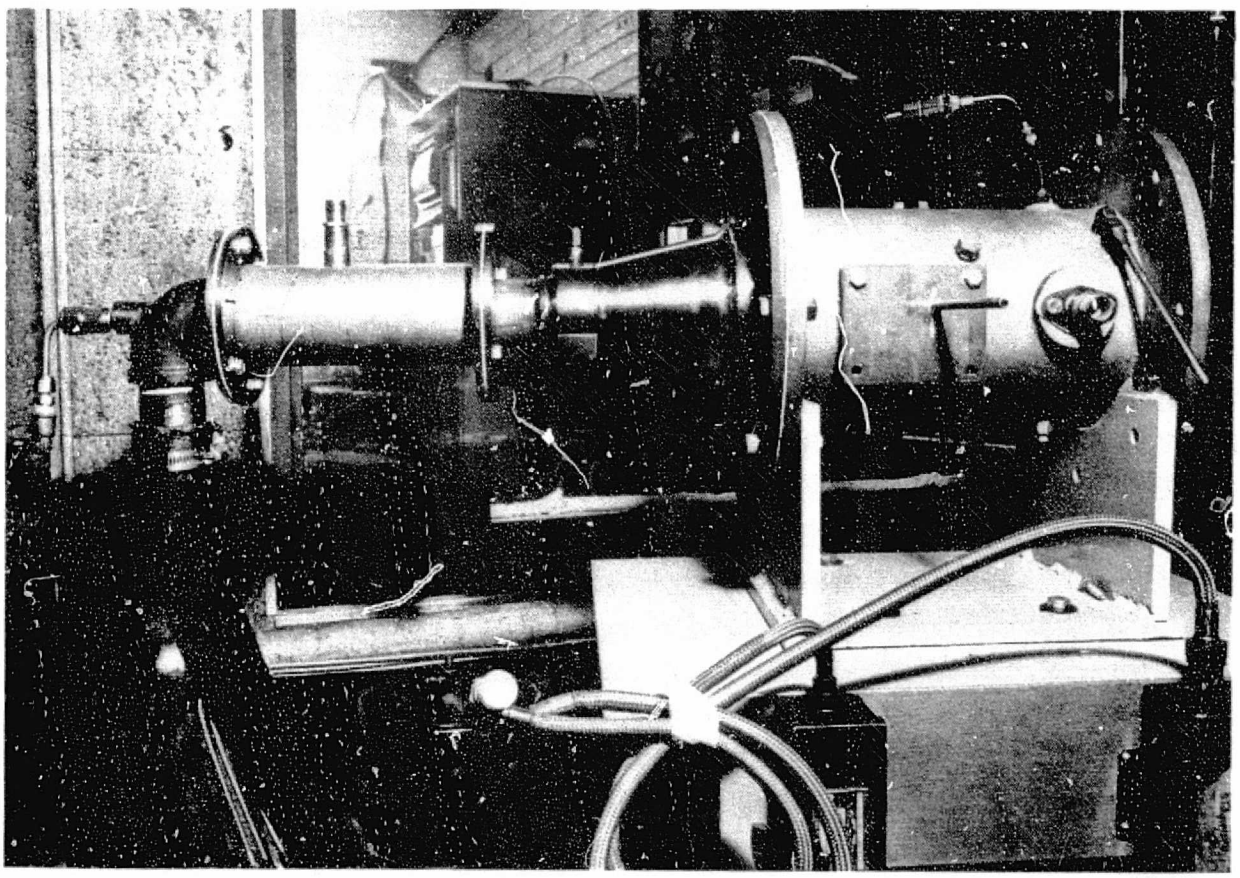

Figure 48. Oxidation/Erosion Rig